TWO DIMENSIONAL LONG WAVE MODELLING

L. Bode, B.Sc., Ph.D. Research Fellow,
Department of Civil & Systems Engineering, James Cook University of North Queensland, Townsville, Q. 4811.

B.A. Harper, B.E., Ph.D. Senior Design Engineer,
Blain, Bremner & Williams Pty. Ltd., 47 Castlemaine Street,
Milton, Q. 4064.

SUMMARY

The aim of this chapter is to describe the techniques of two-dimensional numerical long wave modelling and their application, with interest being focussed on the relatively shallow waters of the continental shelf. Both the equations of motion and associated numerical techniques are described, along with a system of codes to enhance the model's generality and portability. The model is then applied to a portion of the Great Barrier Reef Region of the eastern coast of Australia, to calculate water levels and currents induced both tidally and by the simulated passage of a tropical cyclone.

1. INTRODUCTION

Two-dimensional numerical long wave modelling has its origins two to three decades ago with the pioneering work of Hansen (14), followed by Welander (33), Dronkers (9), Jelesnianski (18), Leendertse (20), Reid and Bodine (22) and Heaps (16). These early models all used basically conventional finite difference (FD) techniques; by and large this is the approach that is still favoured today. In spite of the increasing use of finite elements in many areas of computational mechanics, including long wave modelling (29), it has been argued e.g. by Weare (32) and Thacker (30), that their use in long wave modelling offers no particular advantages and is usually not advised. Accordingly, only (explicit) FD techniques will be addressed in this work, although of course, models can still be formulated in terms of either finite elements or the method of characteristics (31).

The purpose of long wave models is basically twofold: the first is to describe the prevailing dynamics of shallow, usually well-mixed continental shelf waters - this means essentially a description of the tidal and mean wind-induced motions; the second purpose is to describe (and predict) the effect of extreme meteorological forcing on coastal water levels and currents - the storm surge problem. The latter could apply either to high latitude, large-scale storms such as those which inundated the Netherlands and Great Britain in 1953 (and which are the principal reason for the construction of the Thames Barrier) or the smaller-scale but more violent and potentially destructive tropical cyclone storm surge.

The UK Institute of Oceanographic Sciences, in cooperation with the British Meteorological Office has developed an operational storm surge model (21) in which the forcing provided by the predictions of numerical

weather forecast models, in combination with numerical tidal modelling is used to predict coastal water levels around Great Britain. The results of this work, in which the two effects of tides and storm surge are combined *dynamically* (and not simply superimposed) have been shown to be a considerable improvement on earlier estimates and provide a rational basis for evacuation and other counter-disaster procedures.

Roughly 15 years ago, attention was focussed firmly on the tropical cyclone storm surge problem by two major catastrophes. The first was caused by hurricane *Camille*, which crossed the Gulf of Mexico coastline at Bay St. Louis, Mississippi on 17-18 August, 1969. Aircraft penetration of the storm gave a central pressure of 901 mb and the radial extent of the main vortex was small (~ 15 km) with winds gusting up to 300 km/hr. Coastal flooding was most severe at Pass Christian, 10 km east of Bay St. Louis where the storm surge reached 7.4 m (25 ft) above MSL. Total loss of life, due mainly to the storm surge, was 139 and damage was estimated at over $1 billion.

The infamous Bangladesh tropical cyclone of 12-13 November 1970 has been called the "deadliest tropical cyclone in history" (13). The storm tracked northerly in the Bay of Bengal, crossing the Bangladesh coast at the Brahmaputra River delta between Dacca and Chittagong. The intensity of the storm was only moderately extreme (950 to 960 mb) but the peak surge (approximately 4 m) coincided with high tide - mean springs tidal range at Chittagong is 3.5 m. Coastal flooding was extensive in the low-lying, heavily populated delta region. Residents had never experienced such an extreme storm surge and felt no urgency to leave their homes, despite warnings of "Great Danger" from the local Cyclone Warning Service. The consequences were tragic, with an estimated 300 000 people losing their lives. Even the survivors had little fortune, facing a completely devastated local economy with estimates of $63 million in crop losses, 400 000 damaged homes, 300 000 lost cattle and 100 000 boats destroyed.

Roughly one year afterwards, tropical cyclone *Althea* tracked south-west across the Coral Sea, with its centre striking some 50 km to the north of Townsville on Christmas Eve, 1971. There were no fatalities directly attributable to the storm surge, and although there was considerable damage to sea walls, most of the destruction was attributed to wind damage. Yet it is instructive to compare these last two storms. They were very similar (both in central pressure and radial extent) and struck coastlines with almost identical tidal regimes (a range of 3.5 m), with the peak surge above prevailing sea level being roughly 4 m in each case. The Bangladesh storm crossed the coastline at high tide; fortunately for Townsville, Althea's peak was close to the time of low tide. Figure 1 reproduces the measured water level at Townsville and the predicted astronomical tide.

The tropical cyclone storm surge is a meteorologically forced long wave motion resulting in a sustained superelevation of the sea surface, at least for a few hours, above that produced by the normal periodic astronomical tide. It is the result of the combined action on shallow coastal shelf seas of the extreme atmospheric pressure gradients and wind shear stresses generated by a mature tropical cyclone, and can extend over a substantial length of coastline (~ 200 km). The detailed nature of the surge wave at a particular site is sensitive to a number of meteorological and topographical factors, such as the intensity and scale of the tropical

cyclone, the speed and track of the storm, bathymetry, local coastal features (bays, headlands, estuaries) and the astronomical tide. A potentially critical situation arises when the total sustained water level (surge plus tide) exceeds the highest astronomical tide level.

The other major use of two-dimensional modelling has been the accurate description of the astronomical tide in coastal waters. This requires the specification of boundary conditions (usually the amplitude and phase of the various tidal constituents) along the open ocean limits of a modelling region. Such values are usually obtained by direct measurement, although if a small-scale region such as a single bay were being modelled, these values could be obtained by 'nesting' the area of interest within a larger-scale model. If the shelf waters are well-mixed (unstratified), then tidal currents can also be calculated, along with water levels.

Both the authors have been involved in oceanographic work such as tidal modelling in the Great Barrier Reef (GBR) Region and in both the operational and theoretical aspects of tropical cyclone storm surge modelling (15, 24,26). This involvement (for BAH) began with the SURGE storm surge project that followed cyclone *Althea* (24). The basic SURGE model was further modified and extended (by LB) for use in coastal oceanography (3 , 6 , 27). The plan of the remainder of this work is as follows:

§2 describes the equations of motion and other aspects of long wave dynamics, as well as various parameterisation schemes that are required; §3 provides a brief discussion of numerical techniques; §4 describes the application of these modelling techniques to both storm surge and tidal modelling of a portion of the GBR Region; while §5 contains concluding remarks.

2. EQUATIONS OF MOTION

These are the classical long wave or shallow water wave equations describing momentum and mass conservation, with non-linear advective terms retained. They are derived from the Reynolds equations in a rotating frame of reference that have been integrated through the depth of the water column. The vertical equation of motion is reduced to hydrostatic balance, and the assumption is usually also made of constant water density - see e.g. Dronkers (9), Cheng *et al.* (8) for derivations. They have the form:

$$\frac{\partial U}{\partial t} + \frac{\partial}{\partial x}\left(\frac{U^2}{H}\right) + \frac{\partial}{\partial y}\left(\frac{UV}{H}\right) - fV = -H\frac{\partial}{\partial x}\left[g(\eta - \bar{\eta}) + \frac{P_a}{\rho}\right] + \frac{1}{\rho}(\tau_{sx} - \tau_{bx}), \qquad (1)$$

$$\frac{\partial V}{\partial t} + \frac{\partial}{\partial x}\left(\frac{UV}{H}\right) + \frac{\partial}{\partial y}\left(\frac{V^2}{H}\right) + fU = -H\frac{\partial}{\partial y}\left[g(\eta - \bar{\eta}) + \frac{P_a}{\rho}\right] + \frac{1}{\rho}(\tau_{sy} - \tau_{by}), \qquad (2)$$

$$\frac{\partial \eta}{\partial t} + \frac{\partial U}{\partial x} + \frac{\partial V}{\partial y} = 0. \qquad (3)$$

The notation used is:

t	time
x,y	local horizontal Cartesian coordinates
$\eta = \eta(x,y,t)$	sea-surface elevation, referred to a given datum (e.g. M.S.L.)
$\bar{\eta}$	equilibrium tide
$h = h(x,y)$	undisturbed water depth below datum level
$H = h + \eta$	total water depth
f	Coriolis parameter = $2\Omega \sin \phi$ ϕ = latitude, Ω = earth's angular velocity = 7.292×10^{-5} rad/s
g	gravitational acceleration
P_a	atmospheric pressure
ρ	water density, assumed constant
τ_{sx}, τ_{sy}	components of surface stress $\underset{\sim}{\tau}_s$ due to wind forcing
τ_{bx}, τ_{by}	components of bottom stress $\underset{\sim}{\tau}_b$
U,V	components of horizontal transport per unit width of cross section, defined for example, by
$U = \int_{-h}^{\eta} u \, dz$ $= H\bar{u}$	where u is the average velocity and $\bar{u}$ the depth averaged mean velocity, in the x-direction

A similar definition holds for V and $(\bar{v})$.

A barometric effect of spatial variations in P_a is important in tropical cyclone studies, but is otherwise ignored. Direct tidal forcing, through $\bar{\eta}$, is also generally omitted. An exception to this is large-scale ocean tide modelling.

Instantaneous quantities refer in fact to Reynolds averages over the turbulence, typically for several minutes. Nonlinear horizontal advective terms are included in the momentum equations as they cannot necessarily be neglected for surge calculations. The exact form of these terms requires some approximations to be made concerning the vertical velocity distribution, but the form presented can be expected to be an adequate approximation, although probably an under-estimation of magnitudes (33). The equations represent the barotropic ocean response to forcing (wind stress, atmospheric pressure and boundary conditions) with the spatial scales being such that the Coriolis parameter can usually be taken as constant.

2.1 Bottom Stress

The equations can be closed by a suitable parameterization of the bottom stress $\underset{\sim}{\tau}_b$. Common accepted practice is to express $\underset{\sim}{\tau}_b$ in terms of the total transport $q = (U^2 + V^2)^{\frac{1}{2}}$ and total water depth H, by the Darcy-Weisbach or quadratic friction equation, as in quasi-steady open channel

flow - see Task Force Report, ASCE (28)*. For two-dimensional flow,

$$\frac{\underset{\sim}{\tau}_b}{\rho} = \frac{1}{\rho}(\tau_{bx},\tau_{by}) = \frac{\lambda|q|}{H^2}(U,V), \qquad (4)$$

where λ (actually 8λ) is the usual Darcy-Weisbach friction factor. For fully developed turbulent flow, λ is independent of the Reynolds number, but remains dependent on the relative sea bed roughness height in a manner described, for example, by the Colebrook-White formula for an hydraulically rough boundary:

$$\lambda = 8\left\{\log_{10}\left(\frac{14.8H}{k_b}\right)^2\right\}^2 \qquad (5)$$

In the absence of any specific information on bottom roughness, a default value of 0.025 m for the roughness height k_b has been adopted in the authors' work (3, 24, 26, 27). Another common practice is simply to specify λ as a universal constant for a given model, typical values generally lying in the range 0.002-0.003. With k_b = 0.025 m, λ values obtained from Eq. (5) range from 0.0033 down to 0.0014 for depths ranging from 2 m to 100 m - see Figure 2 . Varying either k_b or λ gives scope for tuning a hydrodynamic model should this be considered desirable. Note that in certain circumstances, bottom stress can lag or even oppose the applied surface stress thus leading to potential problems with the application of Eq. (4), which also ignores any Ekman veering in the water column.

2.2 Wind Stress

If wind stress is involved in the forcing then $\underset{\sim}{\tau}_s$ must be specified in terms of the (given) wind field, such as that of a tropical cyclone. Numerous different relations have been proposed in the past, due in part to the inherent difficulties of measurement. The "surface" wind $\underset{\sim}{W}_{10}$ (at height 10 m above M.S.L.) is commonly related to the surface shear stress $\underset{\sim}{\tau}_s$ by the quadratic law, ρ_a being the surface air density:

$$\underset{\sim}{\tau}_s = C_{10}\rho_a|\underset{\sim}{W}_{10}|\underset{\sim}{W}_{10} \qquad (6)$$

There is general agreement that C_{10} is wind speed dependent but the quantitative details remain in dispute. Recent contributions have narrowed the disagreement between formula and data and among formulae, perhaps the simplest of which being that proposed by Wu (34):

$$C_{10} = (0.8 + 0.065\ W_{10}) \times 10^{-3} \qquad (7)$$

---

* This wide-ranging (and readable) discussion of bottom friction does not appear to have had the wide circulation among numerical modellers that it warrants.

for light to hurricane-force winds. The major error source in Eq. (6) for storm surge modelling is, however, not the estimation of C_{10}, but rather the estimation of the complex space and time dependent wind field within a tropical cyclone. Bode and Sobey (5) give a recent discussion of the specification of tropical cyclone surface wind fields.

2.3 Reefs, Flooding, Estuarine Penetration

The continental shelf along Australia's Coral Sea coast is dominated by the 1900 km long GBR, an often near-continuous chain of quite spearate coral reef clusters located along the edge of the continental shelf. The inner fringe of the clusters ranges from 10 km offshore north of Cairns to 150 km offshore between Rockhampton and Mackay, while the outer fringe is typically some 50 km further offshore, beyond which the ocean bed drops rapidly away. These reefs clearly provide some protection from ocean wave penetration from the Coral Sea, as short period waves break on the reefs, dissipating significant energy before reforming inside the inner fringe. The influence of these reefs on long wave penetration, however, is quite different. Wave breaking is unlikely as incident wave lengths are long (of order 100 km for storm tides and even greater for astronomical tides). They most likely act as some form of partial flow barrier, allowing only a relatively small flow over the top in addition to the comparatively unimpeded flow between the individual reefs.

Topographic details of large parts of the reef area are incomplete, but typical dimensions of significant individual reefs are of the order of kilometres, with the reef crests being exposed, in general, at low tide. Accordingly, both coral reefs and other low barriers, such as extensive sandbanks, can be represented as broad-crested weirs in any numerical long wave model. These can be submerged or overflow weirs, or total flow barriers. The actual representation at any particular location and time depends upon the crest elevation of the reef, z_{cr}, with respect to the instantaneous water levels, H_u on the upstream side and H_d on the downstream side of the reef. This is shown schematically in Figure 3, where q is the resulting water discharge per unit width of crest (either U or V, depending on orientation) across the reef. The broad-crested weir equations can be interpreted as steady uniform flow equations, leading to an equivalent bed shear stress and an equivalent friction factor, λ^*. Specifically, for a y-directed barrier,

$$\frac{\tau_{bx}}{\rho} = \lambda^* \frac{|U|U}{(h+\eta)^2} \qquad (8)$$

where

$$\lambda^* = \begin{cases} \dfrac{(h+\eta)^3}{(C_1 \Delta W_1)^2 \Delta s} & \text{(submerged weir)} \\ \dfrac{2(h+\eta)^3}{(C_2 \Delta W_2)^2 \Delta s} & \text{(overflow weir)} \end{cases}$$

and $\Delta W_1 = \frac{1}{2}(H_u + H_d) - z_{cr}$, $\Delta W_2 = H_u - z_{cr}$

are the submerged and overflow weir heads respectively. C_1 and C_2 are discharge coefficients, being approximately $\sqrt{2}$ and 0.5 respectively. Eq. (8) may thus be used directly in the momentum equations to represent the reefs. In the case of z_{cr} greater than both H_u and H_d (a total flow barrier) the conventional coastal boundary condition of no normal flow applies. Applications of this reef parameterisation scheme are made in §4. This model region is centred on Mackay, 400 km to the south of Townsville. The GBR chain is much more dense here as shown in Figure 4. The rectilinear elements represent the reef with z_{cr} = -1 m, while other 'reef' elements, with z_{cr} farther below the surface, model the extensive band of sandbanks at the mouth of Broad Sound.

This approach was first proposed by Reid & Bodine (22), where it was used to provide boundary conditions for Galveston Bay. Recent numerical studies(1,3) indicate that in regions of extensive reefs, the tidal characteristics are sensitive to reef specification, although for the case of storm surges generated by a reasonably intense hurricane, the reef is much more transparent to long waves (24, 25) - see also §4.

Whether or not this reef parameterisation scheme is completely adequate remains an open question, but there appears to be no other approach that is consistent with the requirements of a numerical model. In addition, very little research has been undertaken on the fluid dynamics associated with extensive reef structures. In extensive areas of reef, the weir model, on a regular finite-difference grid, does appear to impose stronger geometric constraints on the flow than might normally be expected to apply in reality. However, recent work, both analytical (17) and numerical (6) suggests that such constraints can be overcome in long wave models of reef regions. The problem is compounded by incomplete information on bathymetry within these large reef structures. Flow across the reef barrier is also sensitive to the specification of reef crest height, and it is difficult to obtain reliable quantitative information on the variation in this parameter, even from experts in reef morphology.

A related problem is that of overbank flooding, since the usual coastal boundary condition of zero normal flow may not be appropriate: the coastal region may be flat rather than an abrupt boundary, thus allowing considerable flooding of water, particularly during a storm surge, across coastal lowlands. A procedure to accomplish this was proposed as an extension of the SURGE model (26). Here, the flood region comprises a two-dimensional cascade of broad-crested weirs and local storages. The concept of local pondage rather than total drying when water levels recede is introduced to overcome the impulsive generation of computational noise that would otherwise be introduced by the 'wet/dry' switching of moving boundary methods. Flather and Heaps (11) use an extension of the moving boundary method, in which more restrictive criteria for the interrogation of grid points for wetting and drying points also leads to a claimed reduction in the generated short scales.

A further consideration arises from the deep penetration of surge or tidal waves into estuaries. Usually, it is not feasible to model such features directly within the context of a two-dimensional model, either by grid nesting or non-uniform grid sizes. The preferred alternative is to interface the two-dimensional model with a one-dimensional estuarine model, such as those described within the present volume. Such a

scheme was also used in association with the SURGE model (26), as depicted in Figure 5 . The estuarine model is denoted by the solid line following the main channels, with branching occurring at the numbered nodal points. Overbank flooding is also incorporated, and coupling is performed through overbank/lateral inflows across the easement boundaries and through the open coast water level and flow histories at the river mouth. Much additional software development is required for such extensions. They are necessary, however, since riverine penetration can be the major component of inland surge propagation, and it is insufficient to consider it simply as a part of the overbank flooding calculations.

2.4 Initial and Boundary Conditions

At coastal boundries, the usual boundary condition is no normal flow:

$$\underset{\sim}{U} \cdot \hat{\underset{\sim}{n}} = 0 \qquad (9)$$

As noted above in §2.3, such a condition may not always be appropriate, particularly in the cases of either significant areas of flooding across coastal lowlands or net inflow from estuarine sources.

It is usual to start computations from the condition of initial quiescence:

$$U = V = \pi = 0, \text{ at } t = 0 \qquad (10)$$

Alternatively should a surge plus tide combined simulation be performed, the appropriate initial condition would be the prevailing astronomical tidal state at that initial instant, over the entire computational region.

The usual assumption made, say for a tidal simulation, is that whatever the result of applied forcing at the initial instant to a computational field (that is possibly unbalanced dynamically), any 'initial transients' so generated will be dissipated ultimately by bottom friction, thus leaving the required forced solution. As discussed by Bode and Sobey (4), initial transients are free computational modes that are encountered in all limited-area long wave numerical models. They are of no physical significance, and indeed are unwanted, but their origin is physical, not numerical. They are initiated by the incompatibility between the usually arbitrary initial conditions and the forcing, which causes an impulsive excitation of the eigenmodes of the limited area model region, an unavoidable situation. To avoid confusion, these free modes will be referred to as 'initial transients', in order to distinguish them from the physical free modes. This is what happens in 'wet/dry' flood codes mentioned above in §2.3. For harmonically forced models (astronomical tide), the forcing is usually supplied by the boundary conditions and, invariably, a settling down time is required to allow the initial transients to be dissipated sufficiently by bottom friction, leaving ultimately the desired forced tidal constituents. For transient models such as the storm surge, where forcing is supplied by the wind stress and pressure gradient fields, both free and forced modes are physically significant, but it is crucial to separate the physical response from the computed free modes.

Thus in certain circumstances, such as very deep water where bottom friction provides insufficient damping, or else in an essentially transient problem such as the passage of a tropical cyclone, special procedures must be adopted to cope with the problem of initial transients.

Either the initiation of forcing in the model must be such as to minimise initial transients, or else they must be able to pass unhindered through the boundaries. Thus initial and boundary conditions are necessarily linked, and it is not always sufficient to adopt the common approach to initial transients, which is simply to ignore them.

In tidal models, it is usual to input the open ocean boundary conditions (and thus, implicitly, the forcing) by specifying there the time history of the tidal signal, preferably from direct measurement and analysis:

$$\eta = \hat{\eta}(t). \tag{11a}$$

Alternatively, the normal component of velocity (or transport) can be similarly specified:

$$\underset{\sim}{U} \cdot \hat{\underset{\sim}{n}} = \hat{U}(t). \tag{11b}$$

The true open coast situation is where major problems arise and where open boundary conditions can exert an identifiable impact on the computed solution. In general there will be two transverse or cross-shelf open boundaries and one basically longshore, in the deep water off the shelf edge. It is usual along the deep ocean boundary to set the free surface elevation η to the pressure surge. Thus:

$$\eta = - \Delta P_a / \rho g. \tag{12}$$

The transverse boundaries are much more difficult to treat, and remain the subject of considerable research effort (7 , 15). The simplest condition is Eq. (12) on transverse open sea boundaries. Obviously this condition will trap energy in the computational region that should, physically, be able to radiate outward. Various authors (12, 18) have suggested that this can be overcome by specifying a condition of zero normal velocity gradient.

Thus, for an x-directed boundary,

$$\partial V / \partial y = 0 \ . \tag{13}$$

However, Reid (23) has pointed out through an attractive argument that Eq. (13) prevents equally the free passage of wave energy through the boundaries. Reid and a number of other workers (10, 21) have advocated the use of a so-called 'radiation' condition. For the simplest case of a one-dimensional channel, it can be shown that if velocity and surface elevation are in phase, then internal reflections are prevented. This leads to the condition:

$$V = \pm c\eta, \tag{14}$$

the sign depending on the direction of the outward normal. The constant of proportionality, c, must have the dimensions of velocity; the default value is the phase speed of free gravity waves, $c = (gh)^{\frac{1}{2}}$, as used by Reid and Bodine (22). This condition is only a partial solution, however. It is not exact if there is any forcing within the region, nor of course can it apply to any forcing external to the region. Its more general application to complex, nonlinear, rotating two-dimensional problems must be viewed cautiously (4). Other boundary conditions based on freely

propagating disturbances or 'Sommerfeld' conditions appear to be enjoying increasingly greater vogue (2, 7). Although they are apparently quite effective and can be applied in conjunction with other forcing such as tidal input (as can Eq. (14)) their origins are basically *ad hoc* and not based on any well-founded physical principles consistent with the equations of motion.

An alternative transverse open boundary condition has been used in the SURGE model (15, 24), termed the Bathystrophic Storm Tide or B.S.T. approximation. Open boundary water levels are set to the local bathystrophic storm tide, the quasi-steady profile along the open boundary, computed on the assumption that the lowest order momentum balance at the boundary is in fact directed along the boundary. Inertial and Coriolis terms are ignored, as is bottom stress. For an x-directed transverse boundary, Eq. (1) reduces to the first order ordinary differential equation:

$$\frac{d\eta}{dx} = -\frac{1}{\rho g}\frac{dP_a}{dx} + \frac{\tau_{sx}}{\rho g(h+\eta)} \quad . \qquad (15)$$

The initial condition in deep water is Eq. (12), and Eq. (15) is integrated into the coast by any standard algorithm such as Runge-Kutta. It readily reproduces wind setup and setdown and has been extensively utilised in the series of SURGE site simulations along Australia's northern coastline. Although superior to Eq. (12) it must still trap wave energy, and for a purely longshore wind field, it does indeed reduce to Eq. (12).

The fact remains, nevertheless, that the problem of successful treatment of open boundary conditions is a long-standing one and to a considerable extent remains unresolved.

One method that deserves further attention is that of nested grid modelling. Here the region of major interest, around the landfalling centre of the storm, is nested within a larger, coarser-meshed region that drives flow in the fine-scale region. This has been implemented with the SURGE model - see Figure 5. At a higher level of sophistication, information could be transmitted into the fine-scale region along the incoming characteristic (4). This specification of the incoming characteristic, without reference to the outgoing characteristic, eliminates all possibility of internal reflections and hence the generation of initial transients. Overall, this method would appear to be satisfactory, provided the large-scale model is global in some sense - i.e. it is not subject to major similar problems on its own boundaries.

2.5 Surge-Tide Interactions

The astronomical tidal background is a further complication in storm tide modelling. As mentioned in the Introduction, the tidal range as well as the state of the tide at landfall are key factors in determining the total surge magnitude and its destructive impact on coastal locations. It has long been realised however, that due to inherent nonlinearities, simple superposition of surge and tide can lead to a significant error in the prediction of both the magnitude and timing of the peak storm tide. In spite of this very little account has been taken of it, and superposition remains common practice. Nevertheless, the result of adding the tide to imposed boundary conditions does appear to have led to a significant

improvement for surge hindcasts in the North Sea (21). This question will be returned to for tropical cyclone modelling in §4 below.

2.6 Simpler Two-Dimensional Models

The major restriction on the early development of two-dimensional models was that of computing resources. This is much less of a problem in the present era, with the advent of super mini-computers such as the VAX 11/700 series putting large-scale 'number crunching' within the reach of many more users. Indeed, fully three-dimensional models are now becoming a realistic proposition. Nevertheless, there exist simpler models than those of the type described here. They are much cheaper to run, computationally, and although they offer a more limited description of the physics, are valuable either for 'first look' exercises or for exploratory numerical experimentation over parameter ranges. Two such models are described here: a linear, single constituent tidal model and a rigid lid wind-driven circulation model - see e.g. Ref. (19).

2.6.1 *Linear Tidal Model*

By removing the nonlinear advection terms, replacing the total depth H by the ambient depth h, and linearising bottom friction, Eqs. (1) - (3) in the absence of wind stress and atmospheric pressure variations reduce to:

$$\frac{\partial U}{\partial t} - fV = - gh \frac{\partial \eta}{\partial x} - \frac{rU}{h} , \qquad (1a)$$

$$\frac{\partial V}{\partial t} + fU = - gh \frac{\partial \eta}{\partial y} - \frac{rV}{h} , \qquad (2a)$$

$$\frac{\partial \eta}{\partial t} + \frac{\partial U}{\partial x} + \frac{\partial V}{\partial y} = 0 \quad . \qquad (3)$$

Here r is the linear friction coefficients (units of velocity). The equilibrium tide $\bar{\eta}$ has been removed, although it can be included if required. If the assumption is then made of forcing by a single tidal constituent, of angular frequency ω, then by letting

$$\eta(x,y,t) = \mathrm{Re} \{\eta_o(x,y)\, e^{i\omega t}\} ,$$

with similar expressions for U and V, where Re{ } denotes the real part of a complex number, the equations can be reduced to a single Helmholtz equation for η_o:

$$\frac{\partial^2 \eta_o}{\partial x^2} + \frac{\partial^2 \eta_o}{\partial y^2} + \kappa^2 \eta_o = 0 \qquad (16)$$

This is the case for constant depth, with κ being a complex function of ω, f, g, h and r. In the more typical case of variable h, Eq. (16) contains additional terms that involve spatial gradients of h. It is still, however, of the same general type, and the same solution techniques apply. Eq. (16) is elliptic and can be solved numerically as a FD problem, given suitable specification of η_o on the boundaries by the

usual methods, either direct (Gaussian elimination) or iterative (e.g. Successive Over-Relaxation). The main advantages are obviously speed and economy; the major disadvantages are limitations on the physical representation of various terms, as well as the fact that forcing is constrained to be a single harmonic component.

2.6.2 *Rigid Lid Circulation Model*

For long-period motion (time scales of the order of weeks) then either an appeal to physical scaling arguments or the use of direct measurements shows that the free surface term in the continuity equation (3) can be ignored, and the transport field (U,V) is effectively non-divergent - the so-called rigid lid approximation. This allows a stream function ψ to be defined, by

$$U = \frac{\partial \psi}{\partial y} \quad , \quad V = - \frac{\partial \psi}{\partial x} \quad , \tag{17}$$

Further, cross-differentiation allows η to be eliminated from the momentum equations (1) and (2), although it can in principle be recovered, if desired. On again replacing H by h, these operations lead to a single (barotropic vorticity) equation for ψ:

$$\left[\left(\frac{\psi_x}{h}\right)_x + \left(\frac{\psi_y}{h}\right)_y\right]_t + f\left[\left(\frac{\psi_x}{h}\right)_y - \left(\frac{\psi_y}{h}\right)_x\right]$$

$$= \frac{1}{\rho} \left\{\left[\left(\frac{\tau_{sx}}{h}\right)_y - \left(\frac{\tau_{sy}}{h}\right)_x\right] - \left[\left(\frac{\tau_{bx}}{h}\right)_y - \left(\frac{\tau_{by}}{h}\right)_x\right]\right\} . \tag{18}$$

Single x, y and t subscripts denote partial derivatives. Wind stress is specified, e.g. by Eqs. (6) and (7), while bottom stress is expressible in terms of ψ through Eqs. (4) and (5). Various conventional FD schemes can be devised for the solution of Eq. (18). The absence of any terms involving the free surface elevation η, means that the highly restrictive CFL limit on the time step (see §3) can be relaxed, to allow values of the order of an hour, rather than a minute to be used (19).

3. NUMERICAL TECHNIQUES

Only a limited discussion of the numerical methods used in the SURGE model will be presented here - they are covered in comprehensive detail by the SURGE report (24) and in other papers that have arisen out of this work (5, 15, 26). In addition, Professor Apelt, elsewhere in this volume, has devoted considerable attention to numerical methods and, in particular, has covered the important questions of numerical accuracy, consistency, convergence and stability.

Much has been written about the details of various numerical solution schemes for Eqs. (1) - (3). However, it is fair to state that, for the long wave equations, the overwhelmingly standard and accepted numerical method has remained explicit finite difference (FD) schemes. In spite of the continued search for more sophisticated methods, it is a relatively simple matter to produce an error-free computer code for an explicit FD model, a bonus that should not readily be overlooked, when compared with other approaches, such as implicit FD or finite elements.

For the present purposes the SURGE FD scheme is described below - see Refs. (15, 24, 26). The flow field, coastal details and offshore bathymetry including features such as reef and coastal flood plains are represented on a square grid of typical unit dimension Δs ($=\Delta x=\Delta y$) of 5 nautical miles - the idealised model test bed of Figure 6 and the Mackay region grid to be used in §4 are typical examples. The numerical integration of Eqs. (1) - (3) by an explicit FD scheme is effected only at discrete spatial and temporal locations ($i\Delta x$, $j\Delta y$, $n\Delta t$). The fields of η, U and V are located on a space and time staggered grid, with η and depths at points $(i,j,n+\frac{1}{2})$, x-directed flows, U, at $(i+\frac{1}{2},j,n)$ and y-directed flows, V, at $(i,j+\frac{1}{2},n)$, where i,j and n have only integer values. This is the familiar Richardson lattice or Arakawa C grid of numerical meteorology. The FD approximation of the continuity equation (3) is centred at (i,j,n), the x-momentum equation (1) at $(i+\frac{1}{2},j,n+\frac{1}{2})$ and the y-momentum equation (2) at $(i,j,+\frac{1}{2},n+\frac{1}{2})$. If the nonlinear advective terms are omitted from the momentum equations, the FD equations utilise the computational 'molecules' shown in Figure 7 .

Thus $\eta_{i,j}^{n+\frac{1}{2}}$ at the new time level $(n+\frac{1}{2})\Delta t$ follows from discretisation of Eq. (3) as

$$\eta_{i,j}^{n+\frac{1}{2}} = \eta_{i,j}^{n-\frac{1}{2}} + \frac{\Delta t}{\Delta s}[(U_{i+\frac{1}{2},j}^{n} - U_{i-\frac{1}{2},j}^{n}) + (V_{i,j+\frac{1}{2}}^{n} - V_{i,j-\frac{1}{2}}^{n})].$$

The treatment of the momentum equations is naturally more complex and a certain amount of averaging is necessary, due to various contributions to the equations being defined at the spatially staggered locations. For instance, the Coriolis term, -fV, at $(i+\frac{1}{2},j,n)$ in Eq. (1) can be written as the arithmetic mean of its nearest four neighbours, while the bed friction term

$$\tau_{bx}/\rho \ , \qquad \text{or} \qquad \frac{\lambda}{\rho}\ \frac{(U^2 + V^2)^{\frac{1}{2}}}{H^2}\ U_{i+\frac{1}{2},j}^{n} \ ,$$

is rewritten, to allow effective centred time differencing, as

$$\left((U_{i+\frac{1}{2},j}^{n-\frac{1}{2}})^2 + (\bar{\bar{V}}_{i+\frac{1}{2},j}^{n-\frac{1}{2}})^2 \right)^{\frac{1}{2}} \ \frac{U_{i+\frac{1}{2},j}^{n+\frac{1}{2}}}{(\bar{H}_{i+\frac{1}{2},j}^{n})^2}$$

Here, $\bar{\bar{V}}$ is identical to the four-term average used in the Coriolis terms, while $\bar{H}$ is the appropriate average for the total depth:

$$\bar{H}_{i+\frac{1}{2},j}^{n} = \frac{1}{2}(h_{i,j} + \eta_{i,j}^{n} + h_{i+1,j} + \eta_{i+1,j}^{n}).$$

This allows second order spatial accuracy to be maintained while, simultaneously, an explicit expression for the predicted x-directed transport $U_{i+\frac{1}{2},j}^{n+\frac{1}{2}}$ can still be obtained from this formulation of the quadratic term. Full centred differencing is possible for the nonlinear horizontal advective terms, expressed in divergence form in Eqs. (1) and (2), and no numerical problems have been encountered using this formulation. Inclusion

of these terms means that the spatial extent of the computational molecules will be larger than indicated in Figure 7 , and reduced forms are therefore necessary adjacent to model boundaries. The full FD equivalent of Eq. (1) is:

$$U^{n+\frac{1}{2}}_{i+\frac{1}{2},j} = U^{n-\frac{1}{2}}_{i+\frac{1}{2},j} - \Delta t \{g\bar{H}^{n}_{i+\frac{1}{2},j} [(\eta^{n}_{i+1,j} - \eta^{n}_{i,j}) + (B^{n}_{i+1,j} - B^{n}_{i,j})]/\Delta s$$

$$- f\bar{\bar{V}}^{n-\frac{1}{2}}_{i+\frac{1}{2},j} - (\tau_{sx}/\rho)^{n}_{i+\frac{1}{2},j} + [(U^{n-\frac{1}{2}}_{i+3/2,j})^2/\bar{H}^{n}_{i+3/2,j} - (U^{n-\frac{1}{2}}_{i-\frac{1}{2},j})^2/\bar{H}^{n}_{i-\frac{1}{2},j}$$

$$+ U^{n-\frac{1}{2}}_{i+\frac{1}{2},j+1} \bar{\bar{V}}^{n-\frac{1}{2}}_{i=\frac{1}{2},j+1}/\bar{H}^{n}_{i+\frac{1}{2},j+1} - U^{n-\frac{1}{2}}_{i+\frac{1}{2},j-1} \bar{\bar{V}}^{n-\frac{1}{2}}_{i+\frac{1}{2},j-1}/\bar{H}^{n}_{i+\frac{1}{2},j-1}]/(2\Delta s)\}$$

$$/\{[1 + \lambda\Delta t]\{(U^{n-\frac{1}{2}}_{i+\frac{1}{2},j})^2 + (\bar{\bar{V}}^{n-\frac{1}{2}}_{i+\frac{1}{2},j})^2\}^{\frac{1}{2}}/(\bar{H}^{n}_{i+\frac{1}{2},j})^2\} .$$

A similar explicit expression applies for $V^{n+\frac{1}{2}}_{i,j+\frac{1}{2}}$. The term 'B' denotes the barometric head, or $P_a/(\rho g)$.

As stated previously, there are a number of numerical questions that must be addressed in order to assess the feasibility and accuracy of a numerical scheme such as that above - these are covered in the SURGE Report (24) but also elsewhere in this volume. The most immediate concern is numerical stability. Analysis on the linear form of Eqs. (1) - (3) shows that the time step Δt is limited for a square grid by the CFL (Courant-Lewy-Friedrichs) criteria:

$$\Delta t < \frac{\Delta s}{(2gh_{max})^{\frac{1}{2}}} , \qquad (19)$$

where h_{max} is the maximum water depth. Physically, this means simply that the fastest surface gravity wave cannot be allowed to propagate further than one grid spacing per time step. Further analysis shows that there are additional time-stepping limitations associated with other terms in the equations of motion, such as friction, Coriolis and horizontal advection. For the most part, however, Eq. (19) is the most stringent restriction and provides a very good guide to the value of Δt that will ultimately be chosen.

It is not enough, however, to rely solely on numerical stability. Implicit FD schemes (20) are popular because they impose no inherent limitation to the size of Δt that can be used - they are absolutely stable. Unfortunately, the fact is often overlooked that accuracy, as represented by Fourier response characteristics (20, 24) - i.e. the ability of the FD scheme to allow propagation of gravity wave without significant distortion of amplitude or phase - is the prime consideration. Indeed, it so happens that acceptable values of Δt for implicit schemes are often not greatly larger than those of explicit schemes, as imposed by Eq. (19). In addition, computational costs per time step are higher for implicit models, and should unusual physical features such as reefs or moving coastlines need to be included, they can become much more difficult to implement.

Typically, FD schemes such as that discussed here, perform satisfactorily in terms of negligible wave deformation, for waves with lengths of order $20\Delta s$ or greater. As an illustration, Figure 8 shows the results of one wave deformation analysis in the SURGE report (24) for the linearised long wave equations that contain the Coriolis terms - bottom friction and horizontal advection have been omitted from this case. $|T|$ and $\arg(T)$ measure the wave amplitude and phase distortion; perfect behaviour would give $|T| = 1$ and $\arg(T) = 0$ over the range of $L/\Delta s$, the wavelength as a multiple of grid spacing. The plot of $|T|$ gives negligible amplitude distortion for the stable case of the Courant number, $Cr = (2gh)^{\frac{1}{2}}\Delta t/\Delta s < 1.0$ - see Eq. (19) - over a realistic range of the effective Coriolis term, but with some distortion for $Cr > 1.0$ and $L/\Delta s < 7$. The plot for $\arg(T)$ shows phase distortion even for $Cr < 1.0$ but only when $L/\Delta s < 10$. For $Cr > 1.0$, distortion in $\arg(T)$ increases, showing acceleration for wavelengths up to $L/\Delta s = 30$. Thus, provided the stability criterion, Eq. (19), is observed, such schemes, even with the inclusion of terms like Coriolis forces, show negligible distortion in the long wave case ($L/\Delta s > 20$). Therefore, no such problems should arise in the modelling of tropical cyclone storm surge with a grid spacing of 5 or even 10 nautical miles. For the case of astronomical tidal calculations, this problem is even more remote, as wavelengths are typically of the order of 1000 km or more.

A cautionary note follows, however, from an examination of Figure 8. The use of such schemes in mass transport calculations, where interest centres on the movement of an isolated (and spatially concentrated) substance, is not advised. In this case, the wavelength of the 'disturbance' will in general be small, down towards the theoretical lowest limit, the Nyquist value of $L/\Delta s = 2$. As can be seen from Figure 8 , the short wavelengths will suffer huge phase distortions. Alternative and more suitable methods have to be applied to this, admittedly, much less numerically tractable problem.

3.1 Specification of Computational Codes

It is a relatively straightforward but tedious matter to set up a numerical hydrodynamic model, based on one particular geographic region. In order, however, to enhance the versatility of a model, it is clearly advantageous that it not be site-specific. This is usually accomplished by use of a system of codes, whereby every computational grid point is assigned a pre-ordained code that will result in the relevant computations for that grid point being performed there. Thus, a code file becomes part of the design procedure for a particular location in the same manner as the setting up of a file of bathymetry, $h_{i,j}$. As illustrations, some of the cases used in SURGE are shown in Figure 9. Three examples are given: Code 0 shows that the numerical solution of all three equations (1) - (3) is required at this location (a normal internal grid point) - Level #3 denotes inclusion of advective terms; Code 13 indicates a Level #2 interior grid point at which advective terms are omitted in each equation, when adjacent to boundaries; Code 15 corresponds to a y-directed land boundary, and so on. A further immediate use of the idea of codes is that computer plots for an arbitrary region can be generated immediately with the appropriate software.

4. A NUMERICAL TEST CASE

The SURGE model is used in this section to simulate both tides and a storm surge separately, as well as their combination in an area of the Great Barrier Reef Region, centred on Mackay (27). This modelling exercise is meant as an illustration of the types of phenomena that can be investigated, as well as the range of output results that are obtainable, by use of the modelling techniques described in the previous two sections. The Mackay area is characterised by particularly high tides, with a springs range of order 10 metres in Broad Sound. As well as large astronomical tides, the area is subject to the passage of tropical cyclones. One such cyclone, with an estimated central pressure of 940 mb, hit Mackay in 1918. A significant component of the damage was due to the effects of storm surge (estimated at over 3.6 m at Mackay) and wave action, with the storm crossing the coast near the time of high tide. The combination of extreme winds and very high surge water levels devastated the town.

In this southern (Mackay) section of the GBR Region, the pattern of the astronomical tides is of considerable scientific and applied interest. Tides are much higher than, and exhibit large phase lags relative to areas to the north and south. Spring tides can have a range of up to 10 metres. Recent numerical studies (1, 3) have lent weight to the hypothesis (first proposed, incidentally, by the maritime explorer Matthew Flinders in 1814), that the reef chain itself plays a key role in the attainment of such large water levels. The area is also subjected to the influence of strong and persistent longshore winds for a large part of the year. In addition, the occasional incidence of the passage of tropical cyclones means that such extreme meteorological forcing and the associated water levels and currents, must be included in any coastal engineering assessment of the area. As stated above, the work to be discussed in this section comprises three parts. The first considers the factors which lead to the large amplification of the semi-diurnal astronomical tides. In particular the role played by the dense reef barrier in the tidal dynamics is considered by means of numerical modelling. The second part of the work considers the effect of the passage of a tropical cyclone through this area. In view of the extremely large water levels that are attainable from each of these forcing mechanisms, the ultimate effect of surge/tide interactions on the total water level and currents could well be considerable and should be incorporated in the design of important coastal engineering works in this area, since variations of fractions of a metre in levels could have significant economic implications. This aspect of the coastal hydrodynamics is often neglected and forms the third part of the study.

The model region is shown in Figure 4 . Both the actual coastline and its model approximation on the square grid of spatial resolution, Δs = 5 n miles are shown. This value allows considerable, although not complete resolution of individual reef elements. The figure also shows the region's bathymetry as well as the model's approximation of the reef structure and submerged barriers, which are represented by the dashed rectilinear elements. For the purposes of comparison of the various results that follow, particular attention will be paid to grid point (5,29) in the mouth of Broad Sound. This is the location of Flat Isles where, in fact, Flinders was moored for two weeks in 1814. This point is in the area of maximum tides as well as surge for the chosen model cyclone. As stated in §3, a number of data files for the region in question, are set up prior

to the simulation. These are basically the bathymetry, or depth, $h_{i,j}$ and the model codes, which delineate the computational region, and indicate the type of computation which is to be performed at a particular point. These constitute the BED file, and are shown along with other extracts from the model output in Figure 10.

4.1 Tidal Model

In the Mackay region, tides are predominantly semi-diurnal. In particular, the M_2 constituent accounts for roughly 50% of the total tidal range, as seen from Table I. As a result, M_2 can be taken as representative of a mean tide over the spring-neap cycle. It should be remembered, however, that total tidal water levels can be up to double these values. The tidal model is driven by imposing the M_2 tide (amplitude and phase) along the three open ocean boundaries. The tidal amplitude is increased from zero to its full value over a build-up period of 6 hours in order to reduce the unwanted effects of initial transients (4).

TABLE I

RANGE OF PRINCIPAL TIDAL CONSTITUENTS (METRES) AT SELECTED LOCATIONS IN THE STUDY AREA, TOGETHER WITH THEIR SUM

Location	M_2	S_2	M_2	K_1	O_1	P_1	Sum
Bowen	1.50	0.61	0.40	0.64	0.34	0.21	3.70
Hook Island	1.72	0.63	0.45	0.71	0.35	0.24	4.10
Mackay	3.36	1.20	0.80	0.76	0.40	0.23	6.75
Broad Sound (McEwin Islet)	4.84	1.42	0.43	0.92	0.42	0.25	9.28
Pt. Clinton	2.74	1.10	0.63	0.64	0.32	0.21	5.64
Bell Cay	2.26	1.20	0.42	0.46	0.32	0.21	4.87
Gladstone [(1,1) in Figure 4]	2.32	0.84	0.53	0.50	0.28	0.16	4.63

At present, there remains some uncertainty about this specification of the open boundary conditions, particularly along the edge of the continental shelf. Obtaining data along this stretch is made difficult by the fact that, apart from Hydrographer's Passage, no approach to the shelf edge can be made from the lagoon. Outside the reef, seas are generally too large for safe and recoverable deployment of instruments. Fortunately, this situation is improving and a recent field experiment to Hydrographer's Passage should help to remedy some of the uncertainties, both in boundary data and reef parameterisation.

Figure 11 shows the results of the M_2 tidal similation. The notable feature is the effect of the 'reef': the relatively large gradients of surface elevation and the large phase change across the central (and densest) portion of the reef chain, indicate considerable flow retardation. The mechanism of tidal amplification can also be seen from this figure. The phases of the resultant tidal streams from the north and south are such that they tend to reinforce each other in the central part of the region. The resulting pattern is essentially a standing wave, with almost uniform phase over this large central portion. The tide subsequently progresses up Broad Sound with considerable further estuarine amplification.

M_2 tidal ellipses are presented in Figure 12 . These show the essential pattern of the tidal streams, while the indicated phase depicts the variation from an essentially progressive wave towards a standing wave pattern. The maximum amplitude of the tidal current is 1.8 ms^{-1} (or roughly 3.5 knots) near grid point (25,32). However, personal observations indicate that for the area of the outer reef, tidal currents of up to 8 knots are not uncommon between individual large reefs.

One major advantage of any numerical model is that key parameters can be changed, effectively at will, in order to assess their relative importance. For example, the effects of the reef on the propagation of the tides can be further demonstrated by the complete removal of the reef elements from the model. The results of this numerical experiment are shown in Figure 13. The amplification of the tides is now much reduced. For example, at grid point (5,29), the M_2 amplitude is reduced from 2.66 m in Figure 11 to 2.01 m in Figure 13 . In addition, the tides are no longer so retarded at the edge of the shelf, and phases as a result, are significantly earlier - by roughly 0.7 h - in the central coastal portion of the model region. The results of this simulation lend strong support to the original Flinders hypothesis of reef retardation leading to longshore lagoonal resonance.

4.2 Storm Surge Simulation

In this study, a simulated tropical cyclone of similar estimated magnitude to the 1918 storm is allowed to pass through the model region along the track indicated in Figure 4 . The actual parameters governing this storm are detailed in Table II.

TABLE II

PHYSICAL PARAMETERS GOVERNING THE SIMULATED TROPICAL CYCLONE OF THIS STUDY

Return Period	500 years
Central Pressure	940 mb
Ambient Pressure	1013 mb
Radius of Max. Winds	30 km
Track (Bearing)	255°
Speed of forward movement	30 kph
Simulation Time	- 10 h to + 1 h
Initial Grid Position	(30.9, 46.1)
Final Grid Position	(0.2, 28.4)
Build-Up Time	4 hours

As with the tidal modelling, the storm is built up in magnitude over a number of hours, in order to minimise the unwanted effects of initial transients. The landfall position and path (Figure 4) have been designed deliberately to cause maximum enhancement of the storm surge in the region of maximum tides (Figure 11). The extensive range of numerical experimentation carried out in the SURGE report (24) showed that the maximum surge for Southern Hemisphere cyclones should be situated a distance of order R, the radius of maximum winds, to the left of the eye at landfall, looking along the track of the storm. Thus both maximum tides and surge should occur around the mouth of Broad Sound, and it is hypothesised that

this should result in a very considerable surge/tide interaction, to be discussed below in §4.3.

Figure 14 shows storm surge water levels for the standard run, at times of t = -8, -4, -2, -1, 0 and +1 hours with respect to the time of landfall. At the chosen point (5,29), the maximum surge is of order 4.3 m, although larger values are obtained farther up Broad Sound. These would have to be treated with some caution, however, as no effort has been made in this case to model lowland flooding, which would result in significant dissipation, compared with the usual coastal 'cliff' condition - Eq. (9) - which has been employed.

Figure 15 shows the development over time of the depth-averaged currents induced by the passage of the cyclone. Longshore currents near time of landfall are particularly intense, and reach a maximum value at roughly t = -2. Peak currents at this time, as seen in Figure 15(d), are of order 1.8 ms^{-1} or $3\frac{1}{2}$ knots.

Figure 16 shows the results of the standard surge simulation, but without the reef elements, at t = -1. When compared with Figure 14(d), it can be seen that, unlike the case of the tides, storm surge water levels (and currents) are effectively insensitive to the presence of even such dense reef as in this model region. Apart from some minor differences, surge levels are almost unchanged by the absence of reef and peak levels are identical. It can be deduced that the transient nature of the rapidly moving cyclone, together with the intensely local nature of the forcing dictates such a response.

4.3 Surge/Tide Interaction

The calculations of the previous two simulations have shown that both the storm surge and tidal phenomena have substantial magnitude in this area, and that these are roughly of the same order. When this is considered along with the non-linearities of Eqs. (1) - (3), it would appear essential to consider the possible effects of surge/tide interactions. In other circumstances, this may not be necessary. For example, if the tide is the dominant effect, then it is possible to linearise the surge equation by appropriate techniques. Here, however, surge and tide are of the same order, but this presents no real difficulty with numerical modelling - boundary conditions and forcing terms from the individual simulation are added. The basic question is whether or not surge plus tide provided a sufficiently accurate estimate of the combined surge/tide simulation, and, if not, by how much does it under-estimate or possibly even over-estimate this?

In spite of such possible considerations, there has been scant attention given in the literature to hurricane surge/astronomical tide interactions, although there are some good reasons for this omission. Hurricanes in the US impact predominantly in the Gulf of Mexico where the astronomical tide is negligible, and hence total water levels are basically provided by the storm surge alone. In the UK and Europe tides are quite significant, particularly in the North Sea region, which has been subject to a number of devastating storm surges. However, these storms are of the mid-latitude variety: they are almost always less intense and slower moving than hurricanes and consequently differ considerably in their hydrodynamic response. The mid-latitude storm surge would appear also to be more

amenable to analytical techniques. Nevertheless, numerical modelling has demonstrated the importance of surge/tide interactions (21), showing that surge hindcasts in the North Sea have been improved quite appreciably by joint consideration of the two effects. There has been some consideration of the problem, but mainly for the case of interaction between a large-scale, mid-latitude storm and a one-dimensional model of the Thames estuary. This has supported observations and statistical analysis that suggests the *net* surge tends to peak on the rising tide but not at high tide. In addition, it appears possible in some circumstances for there to be surge amplification as well as a change in the phase of the surge. The principal nonlinearities occur in the pressure terms $(h+\eta)\nabla\eta$, the horizontal advective terms and quadratic bottom friction. No attempt will be made here to analyse their possible effects. It is clear, however, that they prohibit simple superposition of the surge and tidal waves, and can be expected to lead to changes in propagation characteristics (phase speed) and overall dissipation for the combined surge/tide case.

Figure 17 is a comparison of the sea surface elevation at 1 hour before landfall for the two cases: the sum of surge alone plus tide alone in (a) and the combined surge/tide simulation in (b). At the test position, grid point (5,29), the situation at t = -1 which corresponds closely to the time of maximum surge, has elevations of 6.9 m and 6.1 m respectively. The marked reduction in total water levels for the combined simulation is apparent and is a most significant result.

The net surge at t = -1 is depicted in Figure 18(a). This is obtained by subtracting the tidal elevation at t = -1 from the combined surge/tide elevation at the same time. The elevation at (5,29) is 3.5 m. This result can be compared with the case of surge alone in Figure 14(d) for which the corresponding elevation is over 4.3 m. An alternative representation is shown in Figure 18(b) which is a 'window' view of the central portion of the model region - reefs are omitted for clarity, although they were retained in the simulation. This figure gives the excess elevation obtained from the addition of surge plus tide at t = -1 over the combined surge/tide elevations at the same time. This is obtained by subtracting the elevations of Figure 18(a) from those of Figure 14(d) and provides a measure of the extent to which the surge + tide result is conservative. Figure 19 shows traces or time histories of the elevation and depth-averaged velocity components at (5,29). The clipping of the peaks is artificial and is due to the results of the numerical simulations being sampled much less frequently than the time step. Again, the reduction due to interaction, of both and the velocity, particularly around the time of landfall, is clearly seen.

5. CONCLUDING REMARKS

The aim in this chapter has been to give potential users some idea of the applications of an operational, two-dimensional long wave model. Some effort has been devoted in §2 to theoretical aspects, including the difficult problems of boundary conditions and the generation of unwanted modes. In addition, mention is made of simpler alternative methods of modelling both tidal and wind-driven flows. Numerical details are covered rather briefly in §3, since they receive considerable attention elsewhere in this volume. The application of these modelling techniques to the

cases of both tidal and storm surge forcing comprises §4. One important result that can be drawn from this study is the active role of the GBR chain in tidal amplification. This is an unusual result, since elsewhere in the GBR Region, the reef appears to have a slightly dissipative effect on the tides, although in no way does it appear to act as a significant barrier. Here, by acting as a partial barrier to cross-shelf motion, longshore tidal streams are enhanced, leading to am amplification by the mechanism outlined. Storm surge levels, particularly for a track similar to that of the model storm, would be very high in Broad Sound while longshore currents between there and Mackay would be of such magnitude as to cause possibly significant changes to coastal morphology. Consideration is also directed towards the effects of a quite significant surge/tide interaction on resultant water levels and currents. It is shown that a reduction in total water levels of order 1 metre could occur. For both tidal and storm surge work the use of two-dimensional models is common, even routine, and as seen in the case of the UK's model (21), has developed, along with computing power, to the extent where they can be used operationally in a real time, predictive mode.

6. REFERENCES

APELT, C.J. & RICHTER, N.J. (1983) "Modelling Barrier Reef Tides", *Queensland Division Technical Papers, I.E. Aust.*, Vol. 29, pp. 17-22.

BLUMBERG, A.F. & KANTHA, L.H. (1985) "Open boundary conditions for circulation models", *Journal of Hydraulic Engineering, ASCE*, Vol. 111, pp. 237-255.

BODE, L., MASON, L.B., SOBEY, R.J. & STARK, K.P. (1981) "Hydrodynamic Studies of Water Movements within the Great Barrier Reef Region. I. Preliminary Investigations", Department of Civil & Systems Engineering, James Cook University of North Queensland, Research Bulletin No. CS27.

BODE, L. & SOBEY, R.J. (1984) "Initial transients in long wave computations", *Journal of Hydraulic Engineering, ASCE*, Vol. 110, pp. 1371-1397.

BODE, L. & SOBEY, R.J. (1985) "Hurricane storm surge", in *Physical Processes in Coastal, Shelf and Estuarine Zones*, American Geophysical Union, ed. B.J. Noye (in press).

BODE, L. & MIDDLETON, J.H. (1985) "Modelling Great Barrier Reef tides: northern section" (in preparation).

CHAPMAN, D.C. (1985) "Numerical treatment of cross-shelf open boundaries in a barotropic coastal ocean model", *Journal of Physical Oceanography*, Vol. 15, pp. 1060-1075.

CHENG, R.T., POWELL, T.M. & DILLON, T.M. (1976) "Numerical models of wind-driven circulation in lakes", *Applied Mathematical Modelling*, Vol. 1, pp. 141-159.

DRONKERS, J.J. (1964) "Tidal Computations in Rivers and Coastal Waters", North-Holland, Amsterdam.

FANDRY, C.B. (1981) "Development of a numerical model of tidal and wind-driven circulation in Bass Strait", *Australian Journal of Marine & Freshwater Research*, Vol. 32, pp. 9-29.

FLATHER, R.A. & HEAPS, N.S. (1975) "Tidal Computations for Morecambe Bay", *Geophysical Journal of the Royal Astronomical Society*, Vol. 42, pp. 489-517.

FORRISTALL, G.Z. (1974) "Three-dimensional structure of storm-generated currents", *Journal of Geophysical Research*, Vol. 79, pp. 2721-2729.

FRANK, N.L. & HUSAIN, S.A. (1971) "The deadliest tropical cyclone in history?", *Bulletin of the American Meteorological Society*, Vol. 52, pp. 438-444.

HANSEN, W. (1956) "Theorie zur Errechnung des Wasserstandes und der Stromungen in Randmeeren nebst Anwendungen", *Tellus*, Vol. 8, pp. 287-300.

HARPER, B.A. & SOBEY, R.J. (1983) "Open boundary conditions for open-coast hurricane storm surge", *Coastal Engineering*, Vol. 7, pp. 41-60.

HEAPS, N.S. (1969) "A two-dimensional numerical sea model", *Proceedings of the Royal Society of London*, Vol. A265, pp. 93-137.

HUTHNANCE, J.M. (1985) "Flow across reefs or between islands, and effects on shelf-sea motions", *Continental Shelf Research*, Vol. 4, pp. 709-731.

JELESNIANSKI, C.P. (1965) "A numerical calculation of storm tides induced by a tropical storm impinging on a continental shelf", *Monthly Weather Review*, Vol. 93, pp. 343-358.

KELLY, L.R. & ANDREWS, J.C. (1985) "Numerical models for planning coastal circulation studies", *Proceedings 1985 Australasian Coastal & Ocean Engineering Conference*, Christchurch, N.Z. (in press).

LEENDERTSE, J.J. (1967) "Aspects of a Computational Model for Long Period Water-Wave Propagation", Rand Corp., Santa Monica, RM-5294-PR.

PROCTOR, R. & FLATHER, R.A. (1983) "Routine storm surge forecasting using numerical models: procedures and computer programs for use on the CDC Cyber 205E at the British Meteorological Office", Institute of Oceanographic Sciences, UK, Report No. 167.

REID, R.O. & BODINE, B.R. (1968) "Numerical model for storm surges in Galveston Bay", *Journal of the Waterways and Harbors Division, ASCE*, Vol. 94, pp. 33-57.

REID, R.O. (1975) "Comments on 'Three-dimensional structure of storm-generated currents' by G.Z. Forristall", *Journal of Geophysical Research*, Vol. 80, pp. 1184-1185.

SOBEY, R.J., HARPER, B.A. & STARK, K.P. (1977) "Numerical Simulation of Tropical Cyclone Storm Surge", Dept. of Civil & Systems Engineering, James Cook University of North Qld., Research Bulletin No. CS14.

SOBEY, R.J. & HARPER, B.A. (1977) "Tropical cyclone surge penetration across the Great Barrier Reef", *Proceedings of the Third Australian Coastal & Ocean Engineering Conference, I.E. Aust.*, Melbourne, pp. 58-63.

SOBEY, R.J., HARPER, B.A. & MITCHELL, G.M. (1982) "Numerical modelling of tropical cyclone storm surge", *Civil Engineering Transactions, I.E. Aust.*, Vol. CE24, pp. 151-161.

STARK, K.P., BODE, L. & MASON, L.B. (1985) "Simulation of tides and storm surges in the Great Barrier Reef Region", *Proceedings 19th International Coastal Engineering Conference*, Houston, USA, Sept. 1984, pp. 226-242.

TASK FORCE ON FRICTION FACTORS IN OPEN CHANNELS of the Committee on Hydromechanics of the Hydraulics Division (1963) "Friction factors in open channels", *Journal of the Hydraulics Division, ASCE*, Vol. 89, pp. 97-143.

TAYLOR, C. & DAVIS, J. (1975) "Tidal and Long Wave Propagation - A Finite Element Approach", *Computers and Fluids*, Vol. 3, pp. 125-148.

THACKER, W.C. (1978) "Comparison of finite-element and finite-difference schemes. Part II: two-dimensional gravity wave motion", *Journal of Physical Oceanography*, Vol. 8, pp. 680-689.

TOWNSON, J.M. (1974) "An application of the method of characteristics to tidal calculations in (x-y-t) space", *Journal of Hydraulic Research*, Vol. 12, pp. 499-523.

WEARE, T.J. (1976) "Finite element or finite difference methods for the two-dimensional shallow water equations?", *Computer Methods in Applied Mechanics and Engineering*, Vol. 7, pp. 351-357.

WELANDER, P. (1964) "Numerical prediction of storm surges", *Advances in Geophysics*, Vol. 8, pp. 315-379.

WU, J. (1982) "Wind stress coefficients over sea surface from sea breeze to hurricane", *Journal of Geophysical Research*, Vol. 87, pp. 9704-9706.

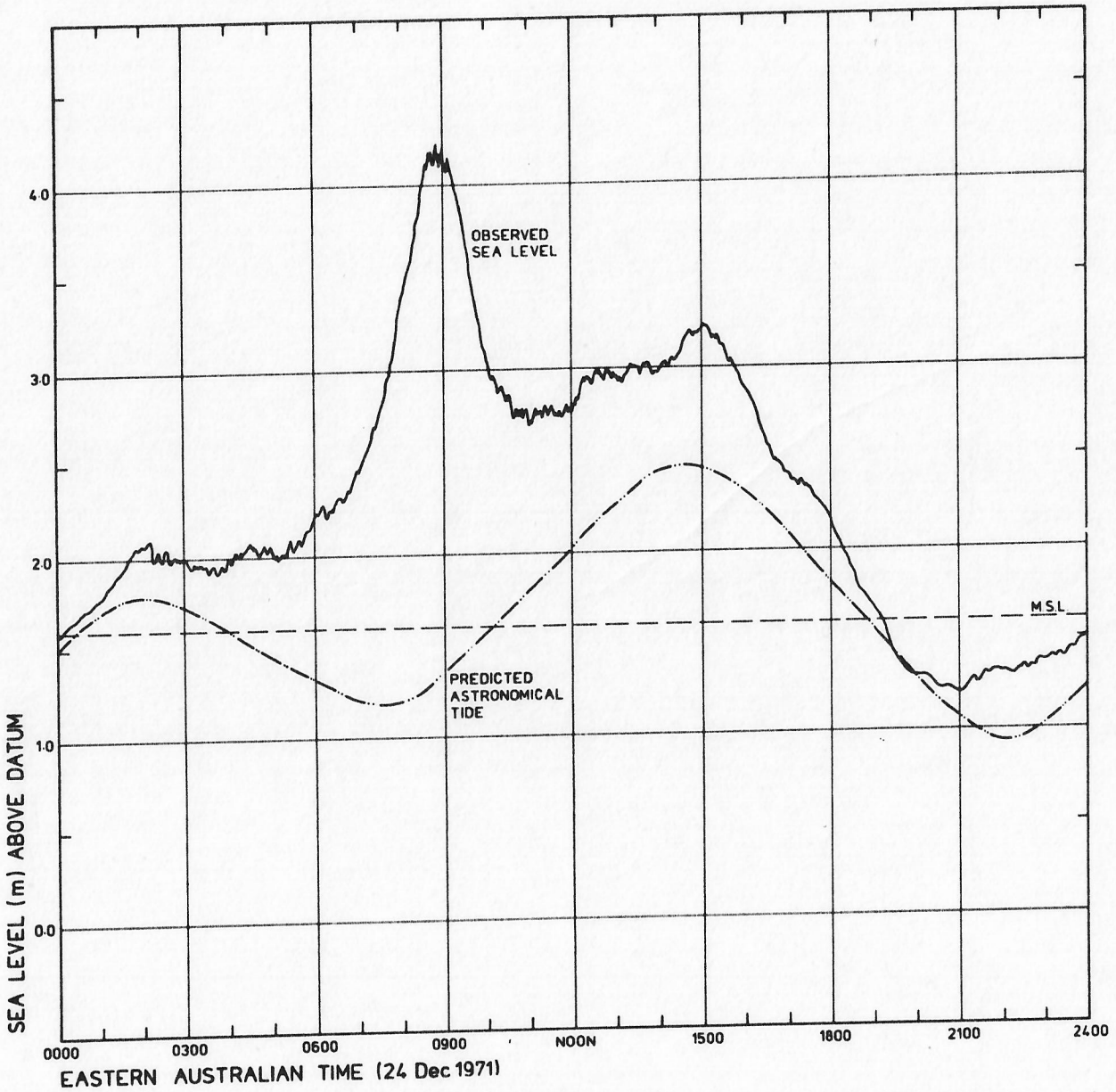

Figure 1. Water level hydrograph at Townsville harbour during tropical cyclone *Althea*. (courtesy of Townsville Harbour Board)

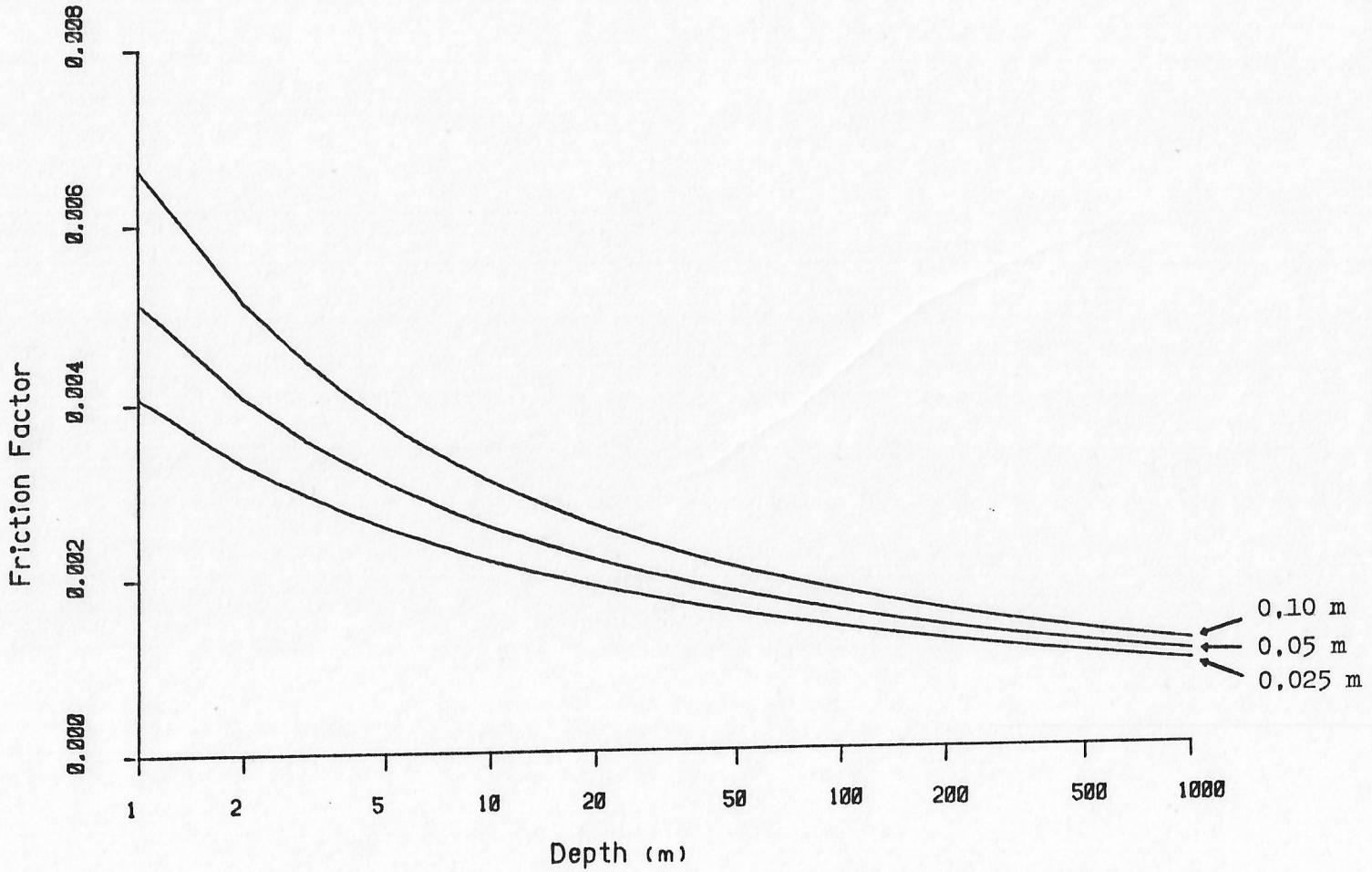

Figure 2. Variation with depth (in metres) of the Darcy-Weisbach friction factor λ, using the Colebrook-White formula, for three values of roughness length, k_b (0.025, 0.05, 0.1 m)

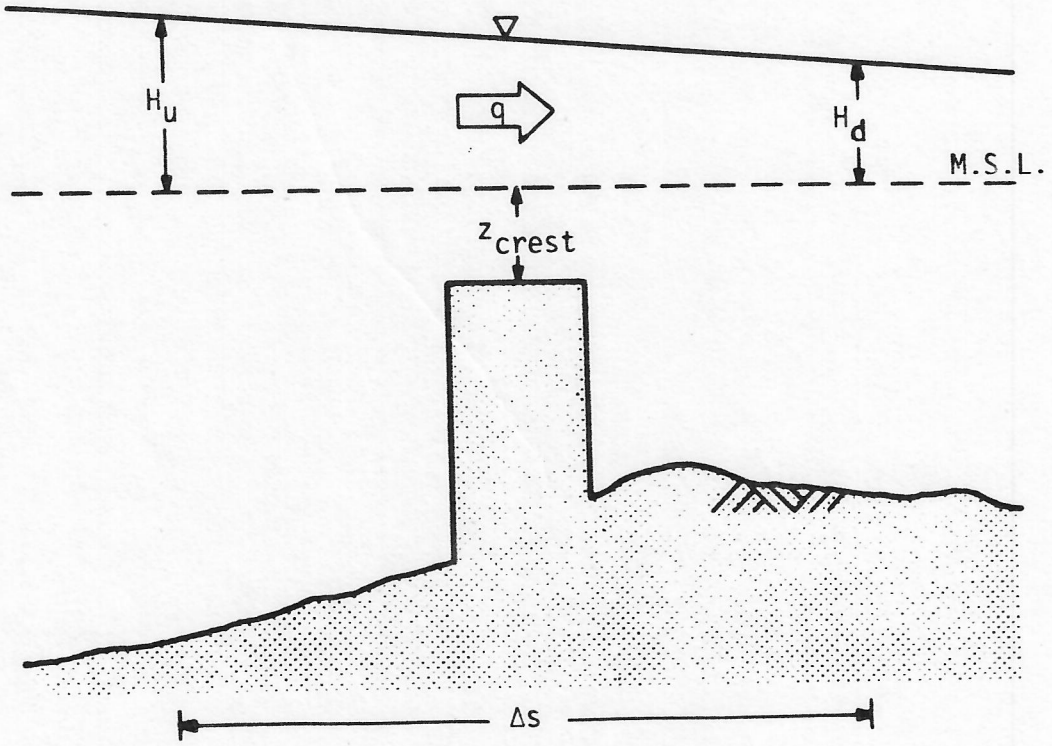

Figure 3: Schematic diagram of a coral reef

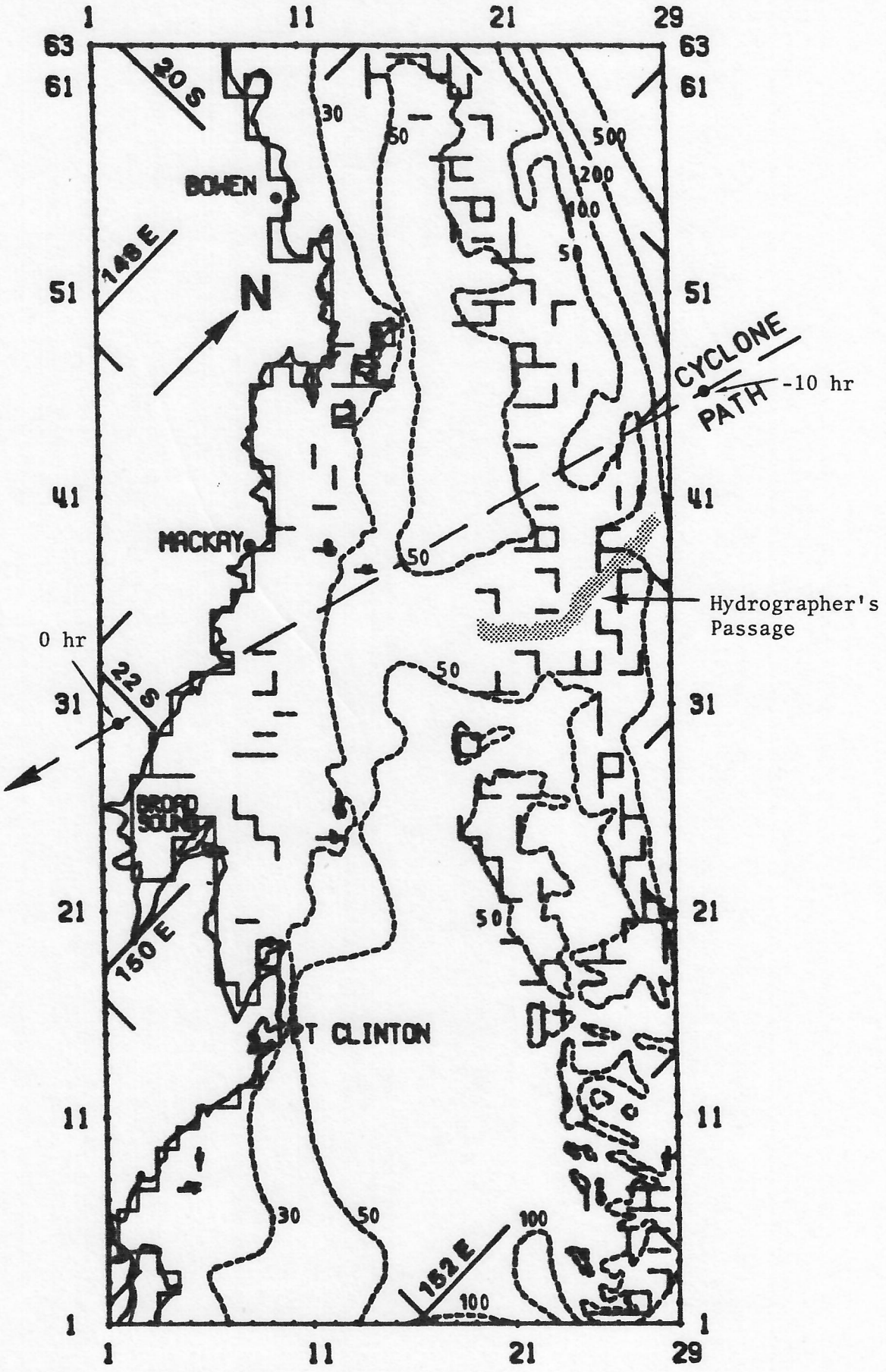

Figure 4. Map of 'Mackay' region, with actual and grid coastlines (Δs = 5 nautical miles) denoted by solid lines. Dashed rectilinear elements denote computational reefs and barriers; dashed contours are isobaths (m). Also indicated are the path of the tropical cyclone's centre plus latitude and longitude at 1° intervals.

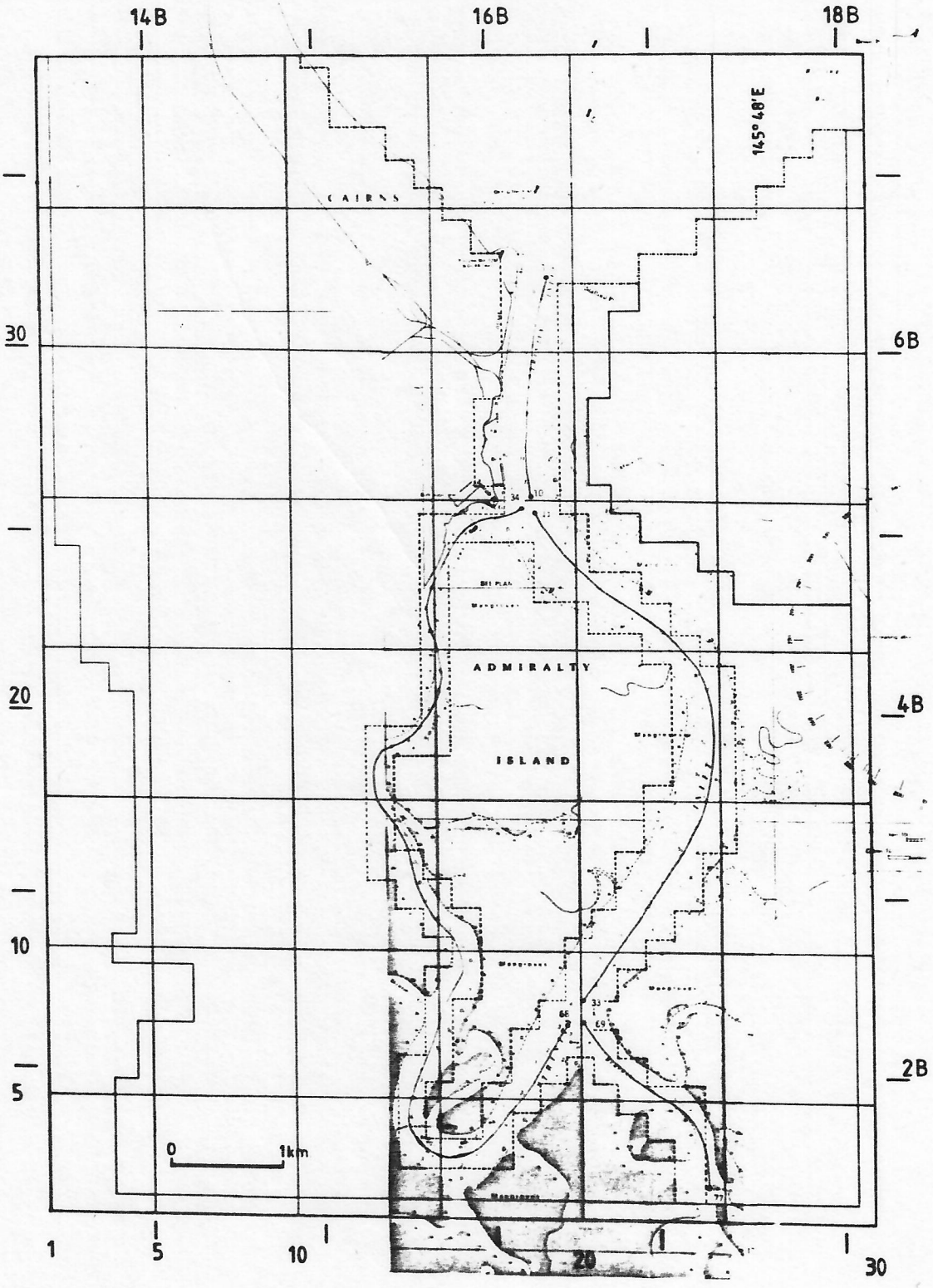

Figure 5. Small scale nested grid (Δs = 257 m) that is linked with a one-dimensional estuarine model, and includes overbank flooding. This is nested within two levels of larger-scale grids (Δs = 1543 m and Δs = 5 n miles), each involving a 6-fold change of scale - see Ref. (26).

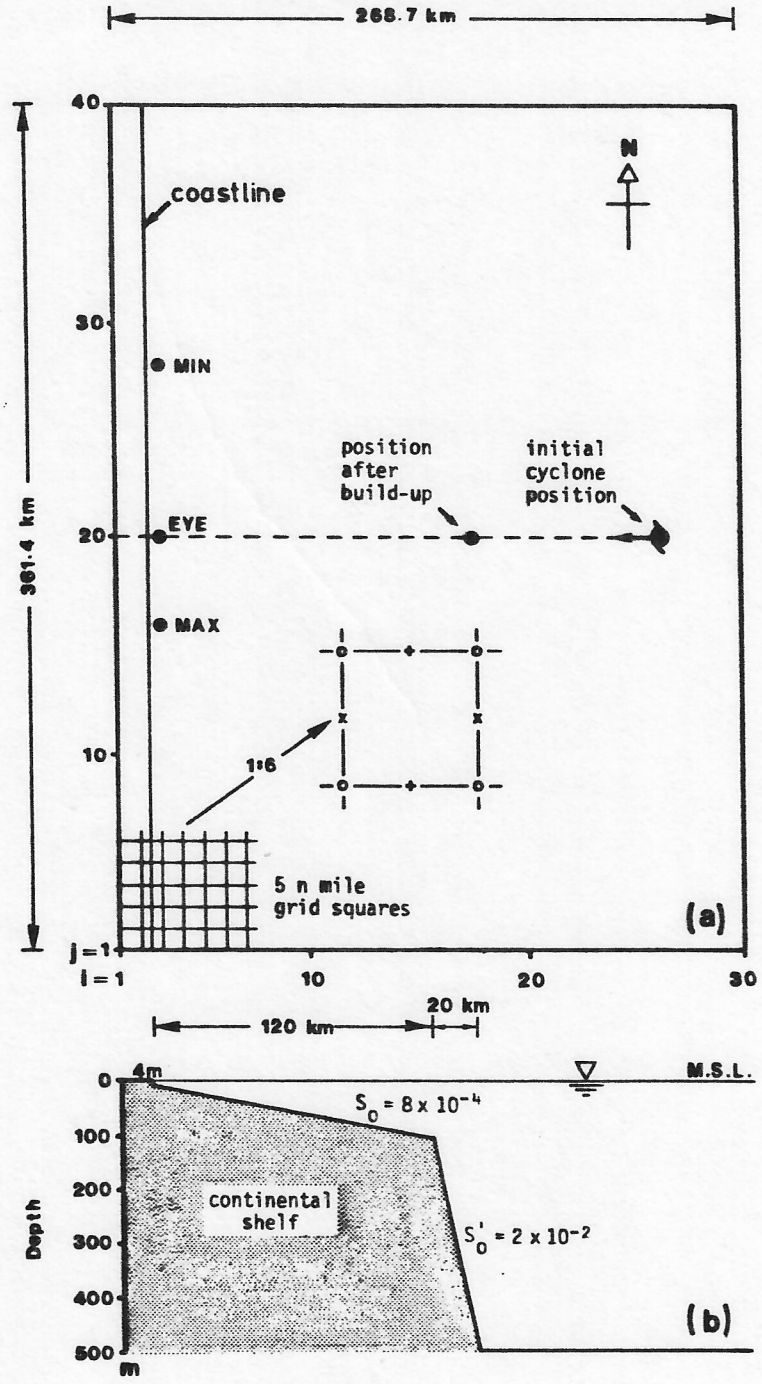

Figure 6. Geometry of the idealised standard model basin, as used in Refs (5,24): (a) number of grid points is 30 x 40 with Δs = 5 n miles, magnified 6-fold to show spatial positioning of η(o), U(+) and V(x) grid points; (b) cross-section of shelf (coastal depth is 4 m) showing bed slopes on the continental shelf and shelf slope.

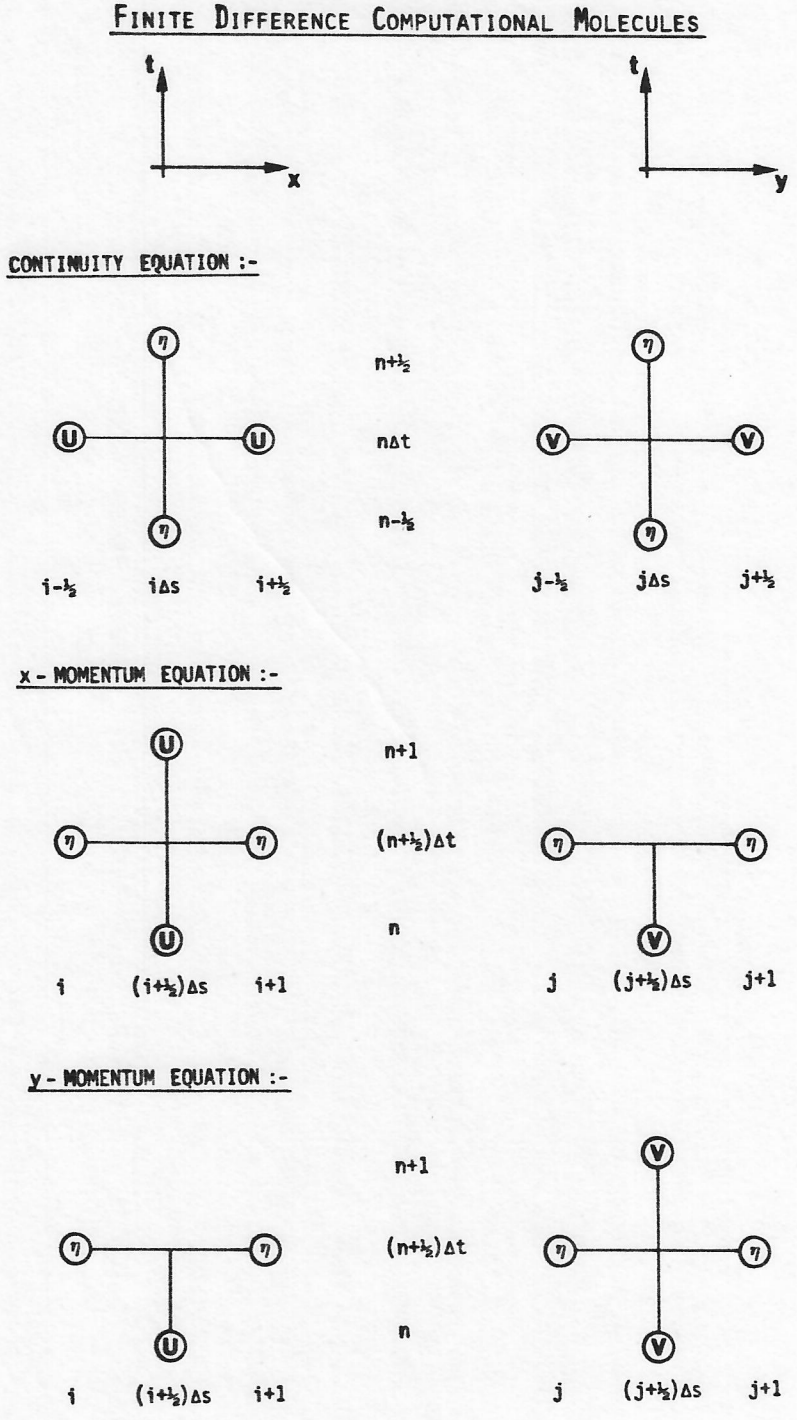

Figure 7. Computational molecules for the numerical solution of Eqs. (1) - (3), without nonlinear advective terms, as described in §3.

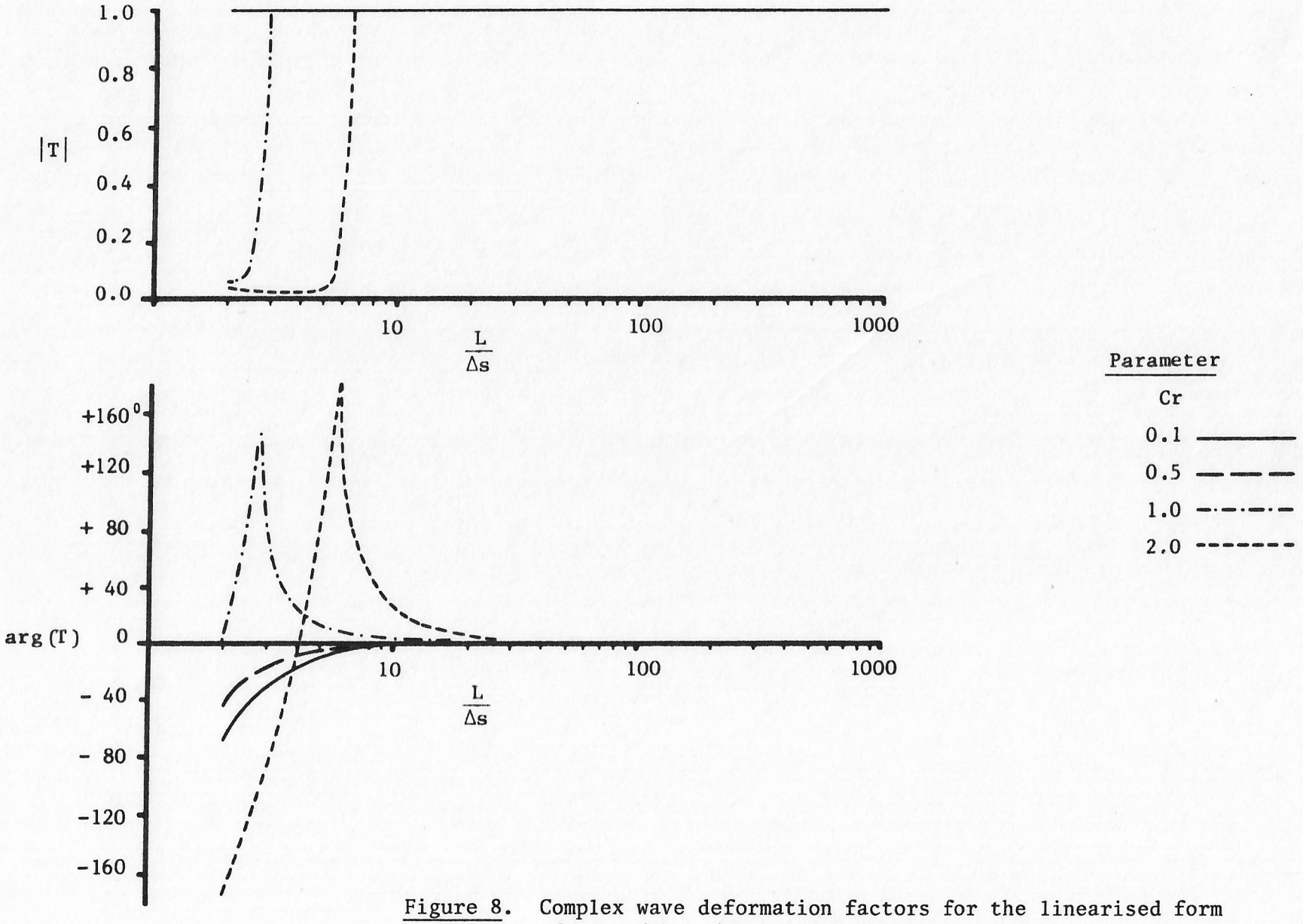

Figure 8. Complex wave deformation factors for the linearised form of Eqs. (1) - (3) including Coriolis terms.

CODE	EXAMPLE	U	V	H
0	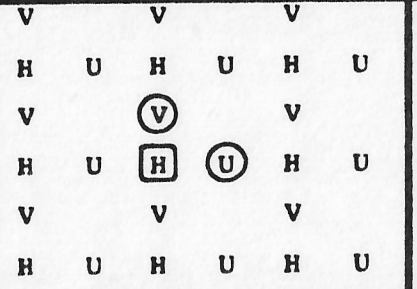	Level #3	Level #3	Continuity
13	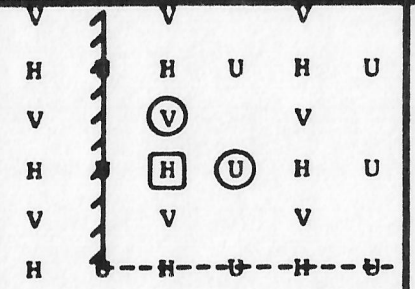	Level #2	Level #2	Continuity
15	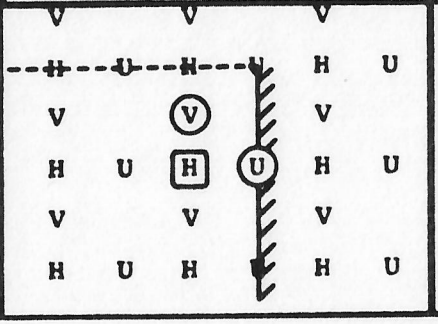	U=0	Level #2	Continuity

Figure 9. Typical model codes for the SURGE model, from Ref. (24).

```
LONG WAVE SIMULATION :  Simulation of storm surge plus tide
--------------------

                                                M2 tidal constituient and Cyclone of 940 mb
                                                High tide and Peak surge timed to occur simultanio

S U R G E :  MAIN0                                                              U S E R :

Department of Civil & Systems Engineering
JAMES COOK UNIVERSITY OF NORTH QUEENSLAND


 RUN DATA :
 --------
          Simulation Date:   IDAY=  1            MONTH=  0            NYEAR=    0
               Start Time:  TBEGIN= 45.00 hr
                Finish Time:   TEND= 90.00 hr
                 Total Time:        45.00 hrs
    Iteration Time Step:   DELT=186.31 s
              Bed Roughness:  ROUGH=2.50E-02 m
  Depth Cut-Off (If App):   DCUT=  -120.00 m
          Ambient Pressure:   PAMB=1013.0 mb                          * default value


 GRID DATA :
 ---------
           Grid Dimensions:   IMAX=  29          JMAX=  63
          Unit Mesh Length:   DELS=  5.00 n mile      =  9.27 km
             Grid Latitude:    PHI= -21.0 deg
              M.S.L. Datum:     HO=   3.0 m
       Grid Angle From North:   PHIG= -45.0 deg
            Input Depth Units:  UNITS=  fath
     Input Land Elevation Units:  UNITS=  m
Reef Crest Elevations (If App): -1.00  -2.00  -5.00
Flood Element Heights (If App):  0.00

      /HOT: flow field initialization from MATC01.SVE
      ----

INITIAL STORM PARAMETERS :
------------------------
          Initial Position of Eye:    CXO= 109.6          CYO=  91.5
          Forward Velocity of Eye:    VFM=   0.0 km/hr  THETFM=   0.0 deg
          Sustained Maximum Winds:    V10= 162.1 m/s     VRMAX= 162.1 m/s   * default value
          Radius to Maximum Winds:      R=  22.7 km                         * default value
             Central Pressure:      PO=   0.0 mb
          Storm Updating Interval:   NCYC=   1 * DELT        = 186.3 s
            Storm Build-up Period:   CBLD=   4.0 hr
```

Figure 10(a). Sample output for combined surge/tide simulation, giving an echo check of model parameters.

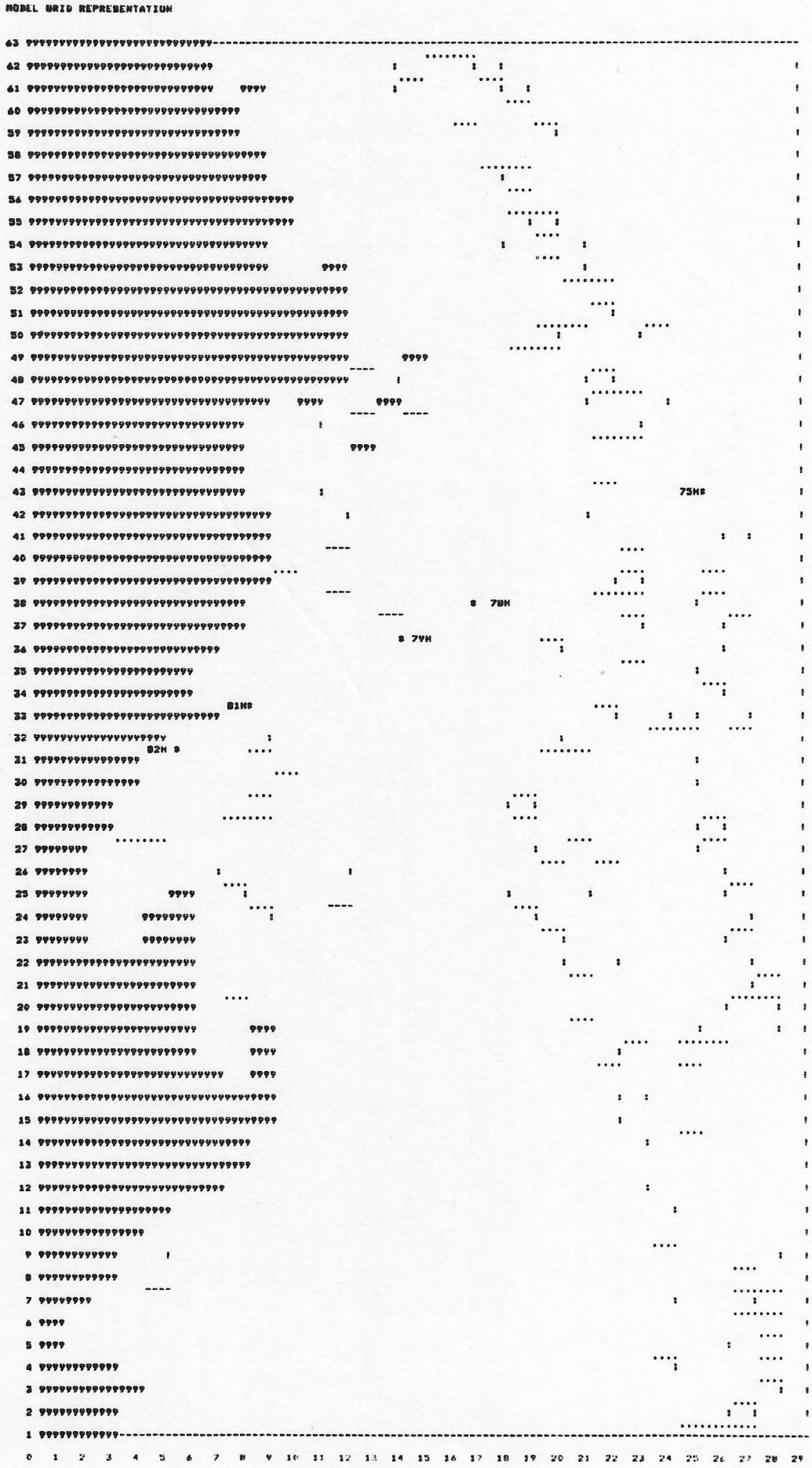

Figure 10(b). Sample lineprinter output of Mackay region, showing reefs (dotted), land (9999) and cyclone path.

```
[21-Aug-84 ] [03:57] [ ECHO ] [MATC20] [   0] [ t21: 0  2th] [ Simulation of storm surge plus tide

INITIAL MODEL DATA :

Boundary Condition Codes for J= 63 to   1 and I=  1 to  29

 63   99  99  99  99  99  99  99   2   2   2   2   2   2   2   2   2   2   2   2   2   2   2   2   2
 62   99  99  99  99  99  99  99  21  21  26  26  26  26-138  26-139-140-138  26  26  26  26  26
 61   99  99  99  99  99  99  99  23  99  21   0   0   0-138-139   0   0-140-138   0   0   0   0   0
 60   99  99  99  99  99  99  99  99  24  26   0   0   0   0   0   0   0   0-139   0   0   0   0   0
 59   99  99  99  99  99  99  99  99  21   0   0   0   0   0   0   0-139   0   0-140   0   0   0   0
 58   99  99  99  99  99  99  99  99  99  21   0   0   0   0   0   0   0   0   0   0   0   0   0
 57   99  99  99  99  99  99  99  99  99  21   0   0   0   0   0   0   0-140-139   0   0   0   0   0
 56   99  99  99  99  99  99  99  99  99  99  21   0   0   0   0   0   0   0-139   0   0   0   0   0
 55   99  99  99  99  99  99  99  99  99  99  21   0   0   0   0   0   0   0-140-140   0   0   0   0
 54   99  99  99  99  99  99  99  99  99  24  21  21   0   0   0   0   0-138   0-139-138   0   0   0
 53   99  99  99  99  99  99  99  99  99  21  23  99  21   0   0   0   0   0   0-139-138   0   0   0
 52   99  99  99  99  99  99  99  99  99  99  99  99  21   0   0   0   0   0   0   0-139-139   0   0
 51   99  99  99  99  99  99  99  99  99  99  99  99  21   0   0   0   0   0   0   0   0-140   0   0
 50   99  99  99  99  99  99  99  99  99  99  99  99  21  22  21   0   0   0   0-140-139   0-138-139
 49   99  99  99  99  99  99  99  99  99  99  99  99  21  23  99  21   0   0-139-139   0   0   0   0
 48   99  99  99  99  99  99  99  99  99  99  99  99  51  50  24  26   0   0   0   0-138-140   0   0
 47   99  99  99  99  99  99  99  99  99  25  99  24  23  99  21   0   0   0   0   0-138-139-139-138
 46   99  99  99  99  99  99  99  99  24  21  53  21  51  24  51   0   0   0   0   0   0   0-138   0
 45   99  99  99  99  99  99  99  99  21   0  21  23  99  21   0   0   0   0   0   0   0-139-139   0
 44   99  99  99  99  99  99  99  99  21   0   0  21  24  26   0   0   0   0   0   0   0   0   0   0
 43   99  99  99  99  99  99  99  99  21  0-338   0   0   0   0   0   0   0   0   0   0-139   0   0
 42   99  99  99  99  99  99  99  99  99  21  0-338   0   0   0   0   0   0   0   0   0-138   0   0   0
 41   99  99  99  99  99  99  99  99  99  21   0  21   0   0   0   0   0   0   0   0   0   0   0   0
 40   99  99  99  99  99  99  99  99  99  21   0  51   0   0   0   0   0   0   0   0   0   0-139   0
 39   99  99  99  99  99  99  99  99  99-339   0  21   0   0   0   0   0   0   0   0   0-138-140   0
 38   99  99  99  99  99  99  99  99  24  26   0  51   0  21   0   0   0   0   0   0   0-139-139   0
 37   99  99  99  99  99  99  99  99  21   0   0   0   0  51   0   0   0   0   0   0   0   0-140   0
 36   99  99  99  99  99  99  99  24  26   0   0   0   0   0   0   0   0   0   0-140   0   0   0   0
 35   99  99  99  99  99  99  24  26   0   0   0   0   0   0   0   0   0   0   0   0   0-139   0
 34   99  99  99  99  99  99  21  21   0   0   0   0   0   0   0   0   0   0   0   0   0   0   0   0
 33   99  99  99  99  99  99  99  21-339   0   0   0   0   0   0   0   0   0   0   0   0-140   0-138
 32   99  99  99  99  99  24  24  26-338   0   0   0   0   0   0   0   0   0   0-138   0   0   0-139
 31   99  99  99  99  24  26   0   0-339   0   0   0   0   0   0   0   0   0   0-139-139   0   0   0
 30   99  99  99  99  21   0   0   0   0-239   0   0   0   0   0   0   0   0   0   0   0   0   0   0
 29   99  99  99  24  26   0   0   0-239   0   0   0   0   0   0   0   0-138-140   0   0   0   0   0
 28   99  99  99  21   0   0   0-239-239   0   0   0   0   0   0   0   0   0-139   0   0   0   0   0
 27   99  99  24-139-139   0   0   0   0   0   0   0   0   0   0   0   0   0-138   0-139   0   0   0
 26   99  99  21   0  22  21-338   0   0   0   0  50  21   0   0   0   0   0   0-139   0-139   0   0
 25   99  99  21  22  23  99  21-340   0   0   0  21   0   0   0   0   0-138   0   0-138   0   0   0
 24   99  99  21  23  99  99  21   0-340   0   0  51   0   0   0   0   0   0-140   0   0   0   0   0
 23   99  99  21  23  99  99  21   0   0   0   0   0   0   0   0   0   0   0   0-140   0   0   0   0
 22   99  99  99  99  99  99  21   0   0   0   0   0   0   0   0   0   0   0   0   0-138   0-138   0   0
 21   99  99  99  99  99  99   0   0   0   0   0   0   0   0   0   0   0   0   0   0   0-139   0   0   0
 20   99  99  99  99  99  99  22-239  21   0   0   0   0   0   0   0   0   0   0   0   0   0   0   0   0
 19   99  99  99  99  99  99  21  23  99  21   0   0   0   0   0   0   0   0   0   0   0   0-139   0   0   0
 18   99  99  99  99  99  99  22  23  99  21   0   0   0   0   0   0   0   0   0   0   0   0   0-138-139   0
 17   99  99  99  99  99  99  99  23  99  21   0   0   0   0   0   0   0   0   0   0   0   0   0-139   0   0
 16   99  99  99  99  99  99  99  99  99  21   0   0   0   0   0   0   0   0   0   0   0   0   0-138-138   0
 15   99  99  99  99  99  99  99  99  99  21   0   0   0   0   0   0   0   0   0   0   0   0   0-138   0   0
 14   99  99  99  99  99  99  99  99  24  26   0   0   0   0   0   0   0   0   0   0   0   0   0   0-138   0
 13   99  99  99  99  99  99  99  99  22   0   0   0   0   0   0   0   0   0   0   0   0   0   0   0   0   0
 12   99  99  99  99  99  99  99  24  26   0   0   0   0   0   0   0   0   0   0   0   0   0   0   0-138   0
 11   99  99  99  99  99  24  24  26   0   0   0   0   0   0   0   0   0   0   0   0   0   0   0   0   0-138
 10   99  99  99  99  24  26   0   0   0   0   0   0   0   0   0   0   0   0   0   0   0   0   0   0   0   0
  9   99  99  99  24  50  21   0   0   0   0   0   0   0   0   0   0   0   0   0   0   0   0   0   0   0-139
  8   99  99  99  21  21   0   0   0   0   0   0   0   0   0   0   0   0   0   0   0   0   0   0   0   0   0
  7   99  99  24  26  51   0   0   0   0   0   0   0   0   0   0   0   0   0   0   0   0   0   0   0   0-138
  6   99  24  26   0   0   0   0   0   0   0   0   0   0   0   0   0   0   0   0   0   0   0   0   0   0   0
  5   99  21  21   0   0   0   0   0   0   0   0   0   0   0   0   0   0   0   0   0   0   0   0   0   0   0
  4   99  99  99  21   0   0   0   0   0   0   0   0   0   0   0   0   0   0   0   0   0   0   0   0   0   0
  3   99  99  99  99  21   0   0   0   0   0   0   0   0   0   0   0   0   0   0   0   0   0   0   0   0-140
  2   99  99  99  24  21  22  22  22  22  22  22  22  22  22  22  22  22  22  22  22  22  22  22  22  22  22
  1   99  99  99   6   6   6   6   6   6   6   6   6   6   6   6   6   6   6   6   6   6   6   6   6   6   6

  0    1   2   3   4   5   6   7   8   9  10  11  12  13  14  15  16  17  18  19  20  21  22  23  24
```

Figure 10(c). Extract of lineprinter output of the pre-defined model codes for the Mackay region - see also Figure 9 ('99' denotes land).

Elevations D to M.S.L. (m) for J= 63 to 1 and I= 1 to 15

63	99.00	99.00	99.00	99.00	99.00	99.00	99.00	-4.83	-19.46	-24.95	-30.43
62	99.00	99.00	99.00	99.00	99.00	99.00	99.00	-12.14	-19.46	-26.77	-32.26
61	99.00	99.00	99.00	99.00	99.00	99.00	99.00	-7.57	99.00	-28.60	-35.92
60	99.00	99.00	99.00	99.00	99.00	99.00	99.00	99.00	-12.14	-24.95	-32.26
59	99.00	99.00	99.00	99.00	99.00	99.00	99.00	99.00	-12.14	-21.29	-30.43
58	99.00	99.00	99.00	99.00	99.00	99.00	99.00	99.00	99.00	-6.66	-28.60
57	99.00	99.00	99.00	99.00	99.00	99.00	99.00	99.00	99.00	-8.49	-19.46
56	99.00	99.00	99.00	99.00	99.00	99.00	99.00	99.00	99.00	99.00	-17.63
55	99.00	99.00	99.00	99.00	99.00	99.00	99.00	99.00	99.00	99.00	-17.63
54	99.00	99.00	99.00	99.00	99.00	99.00	99.00	99.00	99.00	-7.57	-13.97
53	99.00	99.00	99.00	99.00	99.00	99.00	99.00	99.00	99.00	-4.83	-6.66
52	99.00	99.00	99.00	99.00	99.00	99.00	99.00	99.00	99.00	99.00	99.00
51	99.00	99.00	99.00	99.00	99.00	99.00	99.00	99.00	99.00	99.00	99.00
50	99.00	99.00	99.00	99.00	99.00	99.00	99.00	99.00	99.00	99.00	99.00
49	99.00	99.00	99.00	99.00	99.00	99.00	99.00	99.00	99.00	99.00	99.00
48	99.00	99.00	99.00	99.00	99.00	99.00	99.00	99.00	99.00	99.00	99.00
47	99.00	99.00	99.00	99.00	99.00	99.00	99.00	99.00	99.00	-6.66	99.00
46	99.00	99.00	99.00	99.00	99.00	99.00	99.00	99.00	-6.66	-10.32	-17.63
45	99.00	99.00	99.00	99.00	99.00	99.00	99.00	99.00	-12.14	-13.97	-23.12
44	99.00	99.00	99.00	99.00	99.00	99.00	99.00	99.00	-10.32	-17.63	-19.46
43	99.00	99.00	99.00	99.00	99.00	99.00	99.00	99.00	-12.14	-17.63	-15.80
42	99.00	99.00	99.00	99.00	99.00	99.00	99.00	99.00	99.00	-15.80	-17.63
41	99.00	99.00	99.00	99.00	99.00	99.00	99.00	99.00	99.00	-13.97	-17.63
40	99.00	99.00	99.00	99.00	99.00	99.00	99.00	99.00	99.00	-8.49	-13.97
39	99.00	99.00	99.00	99.00	99.00	99.00	99.00	99.00	99.00	-12.14	-13.97
38	99.00	99.00	99.00	99.00	99.00	99.00	99.00	99.00	-10.32	-17.63	-24.95
37	99.00	99.00	99.00	99.00	99.00	99.00	99.00	99.00	-15.80	-21.29	-28.60
36	99.00	99.00	99.00	99.00	99.00	99.00	99.00	-10.32	-15.80	-21.29	-26.77
35	99.00	99.00	99.00	99.00	99.00	99.00	-6.66	-12.14	-15.80	-21.29	-26.77
34	99.00	99.00	99.00	99.00	99.00	99.00	-5.74	-10.32	-13.97	-21.29	-24.95
33	99.00	99.00	99.00	99.00	99.00	99.00	99.00	-15.80	-13.97	-19.46	-24.95
32	99.00	99.00	99.00	99.00	99.00	-4.83	-10.32	-17.63	-12.14	-17.63	-24.95
31	99.00	99.00	99.00	99.00	-5.74	-8.49	-13.97	-15.80	-19.46	-15.80	-21.29
30	99.00	99.00	99.00	99.00	-8.49	-12.14	-12.14	-15.80	-17.63	-17.63	-26.77
29	99.00	99.00	99.00	-6.66	-12.14	-13.97	-17.63	-19.46	-21.29	-23.12	-23.12
28	99.00	99.00	99.00	-8.49	-8.49	-17.63	-17.63	-23.12	-23.12	-24.95	-23.12
27	99.00	99.00	-4.83	-13.06	-19.46	-19.46	-13.97	-17.63	-23.12	-21.29	-23.12
26	99.00	99.00	-13.06	-13.97	-17.63	-10.32	-12.14	-15.80	-23.12	-23.12	-23.12
25	99.00	99.00	-12.14	-12.14	-8.49	99.00	-10.32	-17.63	-10.32	-19.46	-32.26
24	99.00	99.00	-10.32	-8.49	99.00	99.00	-11.23	-17.63	-8.49	-23.12	-34.09
23	99.00	99.00	-5.74	-5.74	99.00	99.00	-8.49	-21.29	-24.95	-23.12	-35.92
22	99.00	99.00	99.00	99.00	99.00	99.00	-11.23	-23.12	-17.63	-21.29	-24.95
21	99.00	99.00	99.00	99.00	99.00	99.00	-13.06	-4.83	-17.63	-32.26	-35.92
20	99.00	99.00	99.00	99.00	99.00	99.00	-12.14	-17.63	-21.29	-32.26	-37.75
19	99.00	99.00	99.00	99.00	99.00	99.00	-13.06	-11.23	99.00	-30.43	-48.72
18	99.00	99.00	99.00	99.00	99.00	99.00	-5.74	-10.32	99.00	-28.60	-48.72
17	99.00	99.00	99.00	99.00	99.00	99.00	99.00	-6.66	99.00	-21.29	-52.38
16	99.00	99.00	99.00	99.00	99.00	99.00	99.00	99.00	99.00	-30.43	-54.21
15	99.00	99.00	99.00	99.00	99.00	99.00	99.00	99.00	99.00	-43.23	-54.21
14	99.00	99.00	99.00	99.00	99.00	99.00	99.00	99.00	-21.29	-43.23	-54.21
13	99.00	99.00	99.00	99.00	99.00	99.00	99.00	99.00	-37.75	-45.06	-52.38
12	99.00	99.00	99.00	99.00	99.00	99.00	99.00	-34.09	-39.58	-45.06	-56.04
11	99.00	99.00	99.00	99.00	99.00	-10.32	-24.95	-34.09	-32.26	-45.06	-56.04
10	99.00	99.00	99.00	99.00	-8.49	-17.63	-26.77	-34.09	-37.75	-43.23	-52.38
9	99.00	99.00	99.00	-6.66	-10.32	-19.46	-24.95	-28.60	-35.92	-41.40	-52.38
8	99.00	99.00	99.00	-10.32	-8.49	-23.12	-30.43	-34.09	-37.75	-43.23	-50.55
7	99.00	99.00	-8.49	-10.32	-17.63	-21.29	-26.77	-30.43	-34.09	-43.23	-46.89
6	99.00	-4.83	-6.66	-15.80	-21.29	-24.95	-28.60	-34.09	-39.58	-41.40	-43.23
5	99.00	-5.74	-10.32	-17.63	-23.12	-28.60	-30.43	-35.92	-34.09	-43.23	-34.09
4	99.00	99.00	99.00	-6.66	-26.77	-30.43	-32.26	-37.75	-39.58	-45.06	-46.89
3	99.00	99.00	99.00	99.00	-24.95	-34.09	-34.09	-35.92	-41.40	-45.06	-43.23
2	99.00	99.00	99.00	-10.32	-26.77	-30.43	-34.09	-35.92	-39.58	-45.06	-46.89
1	99.00	99.00	99.00	-17.63	-26.77	-32.26	-32.26	-24.95	-43.23	-39.58	-48.72
	1	2	3	4	5	6	7	8	9	10	11

Figure 10(d). Extract of lineprinter output of depth (h_{ij}) input file for Mackay region (depth of +99.00 denotes land).

Bed Friction Coefficients (times 1/8) for J= 63 to 1 and I= 1 to 15

63	0.0000	0.0000	0.0000	0.0000	0.0000	0.0000	0.0000	0.0026	0.0019	0.0018	0.0017
62	0.0000	0.0000	0.0000	0.0000	0.0000	0.0000	0.0000	0.0021	0.0019	0.0018	0.0017
61	0.0000	0.0000	0.0000	0.0000	0.0000	0.0000	0.0000	0.0023	0.0000	0.0017	0.0017
60	0.0000	0.0000	0.0000	0.0000	0.0000	0.0000	0.0000	0.0000	0.0021	0.0018	0.0017
59	0.0000	0.0000	0.0000	0.0000	0.0000	0.0000	0.0000	0.0000	0.0021	0.0019	0.0017
58	0.0000	0.0000	0.0000	0.0000	0.0000	0.0000	0.0000	0.0000	0.0000	0.0024	0.0017
57	0.0000	0.0000	0.0000	0.0000	0.0000	0.0000	0.0000	0.0000	0.0000	0.0023	0.0019
56	0.0000	0.0000	0.0000	0.0000	0.0000	0.0000	0.0000	0.0000	0.0000	0.0000	0.0019
55	0.0000	0.0000	0.0000	0.0000	0.0000	0.0000	0.0000	0.0000	0.0000	0.0000	0.0019
54	0.0000	0.0000	0.0000	0.0000	0.0000	0.0000	0.0000	0.0000	0.0000	0.0023	0.0020
53	0.0000	0.0000	0.0000	0.0000	0.0000	0.0000	0.0000	0.0000	0.0000	0.0026	0.0024
52	0.0000	0.0000	0.0000	0.0000	0.0000	0.0000	0.0000	0.0000	0.0000	0.0000	0.0000
51	0.0000	0.0000	0.0000	0.0000	0.0000	0.0000	0.0000	0.0000	0.0000	0.0000	0.0000
50	0.0000	0.0000	0.0000	0.0000	0.0000	0.0000	0.0000	0.0000	0.0000	0.0000	0.0000
49	0.0000	0.0000	0.0000	0.0000	0.0000	0.0000	0.0000	0.0000	0.0000	0.0000	0.0000
48	0.0000	0.0000	0.0000	0.0000	0.0000	0.0000	0.0000	0.0000	0.0000	0.0000	0.0000
47	0.0000	0.0000	0.0000	0.0000	0.0000	0.0000	0.0000	0.0000	0.0000	0.0024	0.0000
46	0.0000	0.0000	0.0000	0.0000	0.0000	0.0000	0.0000	0.0000	0.0024	0.0022	0.0019
45	0.0000	0.0000	0.0000	0.0000	0.0000	0.0000	0.0000	0.0000	0.0021	0.0020	0.0018
44	0.0000	0.0000	0.0000	0.0000	0.0000	0.0000	0.0000	0.0000	0.0022	0.0019	0.0019
43	0.0000	0.0000	0.0000	0.0000	0.0000	0.0000	0.0000	0.0000	0.0021	0.0019	0.0020
42	0.0000	0.0000	0.0000	0.0000	0.0000	0.0000	0.0000	0.0000	0.0000	0.0020	0.0019
41	0.0000	0.0000	0.0000	0.0000	0.0000	0.0000	0.0000	0.0000	0.0000	0.0020	0.0019
40	0.0000	0.0000	0.0000	0.0000	0.0000	0.0000	0.0000	0.0000	0.0000	0.0023	0.0020
39	0.0000	0.0000	0.0000	0.0000	0.0000	0.0000	0.0000	0.0000	0.0000	0.0021	0.0020
38	0.0000	0.0000	0.0000	0.0000	0.0000	0.0000	0.0000	0.0000	0.0022	0.0019	0.0018
37	0.0000	0.0000	0.0000	0.0000	0.0000	0.0000	0.0000	0.0000	0.0020	0.0019	0.0017
36	0.0000	0.0000	0.0000	0.0000	0.0000	0.0000	0.0000	0.0022	0.0020	0.0019	0.0018
35	0.0000	0.0000	0.0000	0.0000	0.0000	0.0000	0.0024	0.0021	0.0020	0.0019	0.0018
34	0.0000	0.0000	0.0000	0.0000	0.0000	0.0000	0.0025	0.0022	0.0020	0.0019	0.0018
33	0.0000	0.0000	0.0000	0.0000	0.0000	0.0000	0.0000	0.0020	0.0020	0.0019	0.0018
32	0.0000	0.0000	0.0000	0.0000	0.0000	0.0026	0.0022	0.0019	0.0021	0.0019	0.0018
31	0.0000	0.0000	0.0000	0.0000	0.0025	0.0023	0.0020	0.0020	0.0019	0.0020	0.0019
30	0.0000	0.0000	0.0000	0.0000	0.0023	0.0021	0.0021	0.0020	0.0019	0.0019	0.0018
29	0.0000	0.0000	0.0000	0.0024	0.0021	0.0020	0.0019	0.0019	0.0019	0.0018	0.0018
28	0.0000	0.0000	0.0000	0.0023	0.0023	0.0019	0.0019	0.0018	0.0018	0.0018	0.0018
27	0.0000	0.0000	0.0026	0.0021	0.0019	0.0019	0.0020	0.0019	0.0018	0.0019	0.0018
26	0.0000	0.0000	0.0021	0.0020	0.0019	0.0022	0.0021	0.0020	0.0018	0.0018	0.0018
25	0.0000	0.0000	0.0021	0.0021	0.0023	0.0000	0.0022	0.0019	0.0022	0.0019	0.0017
24	0.0000	0.0000	0.0022	0.0023	0.0000	0.0000	0.0021	0.0019	0.0023	0.0018	0.0017
23	0.0000	0.0000	0.0025	0.0025	0.0000	0.0000	0.0023	0.0019	0.0018	0.0018	0.0017
22	0.0000	0.0000	0.0000	0.0000	0.0000	0.0000	0.0021	0.0018	0.0019	0.0019	0.0018
21	0.0000	0.0000	0.0000	0.0000	0.0000	0.0000	0.0021	0.0026	0.0019	0.0017	0.0017
20	0.0000	0.0000	0.0000	0.0000	0.0000	0.0000	0.0021	0.0019	0.0019	0.0017	0.0017
19	0.0000	0.0000	0.0000	0.0000	0.0000	0.0000	0.0021	0.0021	0.0000	0.0017	0.0016
18	0.0000	0.0000	0.0000	0.0000	0.0000	0.0000	0.0025	0.0022	0.0000	0.0017	0.0016
17	0.0000	0.0000	0.0000	0.0000	0.0000	0.0000	0.0000	0.0024	0.0000	0.0019	0.0015
16	0.0000	0.0000	0.0000	0.0000	0.0000	0.0000	0.0000	0.0000	0.0000	0.0017	0.0015
15	0.0000	0.0000	0.0000	0.0000	0.0000	0.0000	0.0000	0.0000	0.0000	0.0016	0.0015
14	0.0000	0.0000	0.0000	0.0000	0.0000	0.0000	0.0000	0.0000	0.0019	0.0016	0.0015
13	0.0000	0.0000	0.0000	0.0000	0.0000	0.0000	0.0000	0.0000	0.0017	0.0016	0.0015
12	0.0000	0.0000	0.0000	0.0000	0.0000	0.0000	0.0000	0.0017	0.0016	0.0016	0.0015
11	0.0000	0.0000	0.0000	0.0000	0.0000	0.0022	0.0018	0.0017	0.0017	0.0016	0.0015
10	0.0000	0.0000	0.0000	0.0000	0.0023	0.0019	0.0018	0.0017	0.0017	0.0016	0.0015
9	0.0000	0.0000	0.0000	0.0024	0.0022	0.0019	0.0018	0.0017	0.0017	0.0016	0.0015
8	0.0000	0.0000	0.0000	0.0022	0.0023	0.0018	0.0017	0.0017	0.0017	0.0016	0.0016
7	0.0000	0.0000	0.0023	0.0022	0.0019	0.0019	0.0018	0.0017	0.0017	0.0016	0.0016
6	0.0000	0.0026	0.0024	0.0020	0.0019	0.0018	0.0017	0.0017	0.0016	0.0016	0.0016
5	0.0000	0.0025	0.0022	0.0019	0.0018	0.0017	0.0017	0.0017	0.0017	0.0016	0.0017
4	0.0000	0.0000	0.0000	0.0024	0.0018	0.0017	0.0017	0.0017	0.0016	0.0016	0.0016
3	0.0000	0.0000	0.0000	0.0000	0.0018	0.0017	0.0017	0.0017	0.0016	0.0016	0.0016
2	0.0000	0.0000	0.0000	0.0022	0.0018	0.0017	0.0017	0.0017	0.0016	0.0016	0.0016
1	0.0000	0.0000	0.0000	0.0019	0.0018	0.0017	0.0017	0.0018	0.0016	0.0016	0.0016
	1	2	3	4	5	6	7	8	9	10	11

Figure 10(e). Extract of calculated friction factors [see Eqs. (4), (5)] for Mackay region - $\lambda = 0$ denotes a land point.

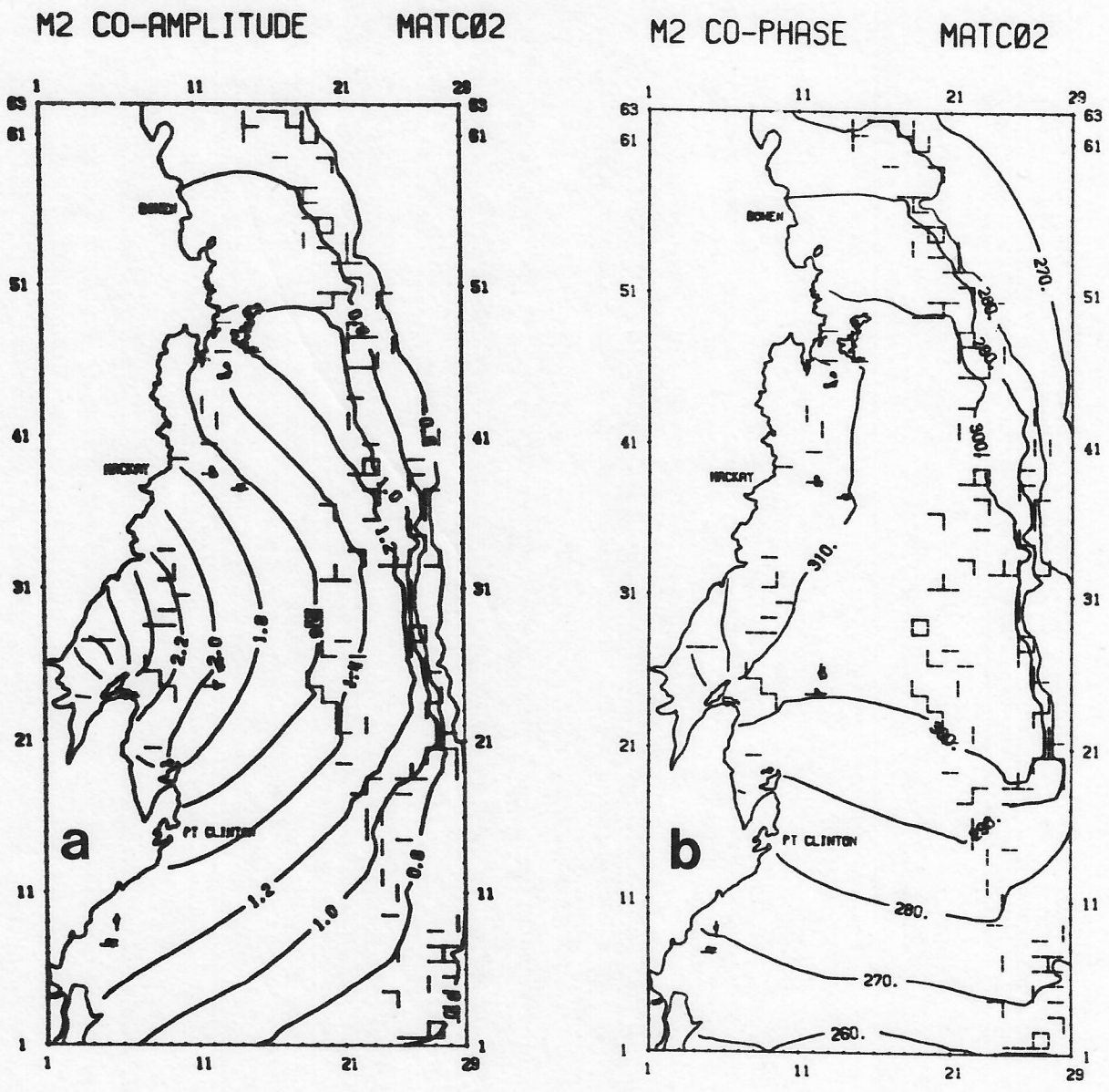

Figure 11. (a) Contour plots of co-amplitude (metres) and (b) co-phase (g degrees) for modelled M_2 tide in Mackay region. Grid spacing, Δs, is 5 nautical miles; rectilinear dashed elements depict reefs and other submerged barriers.

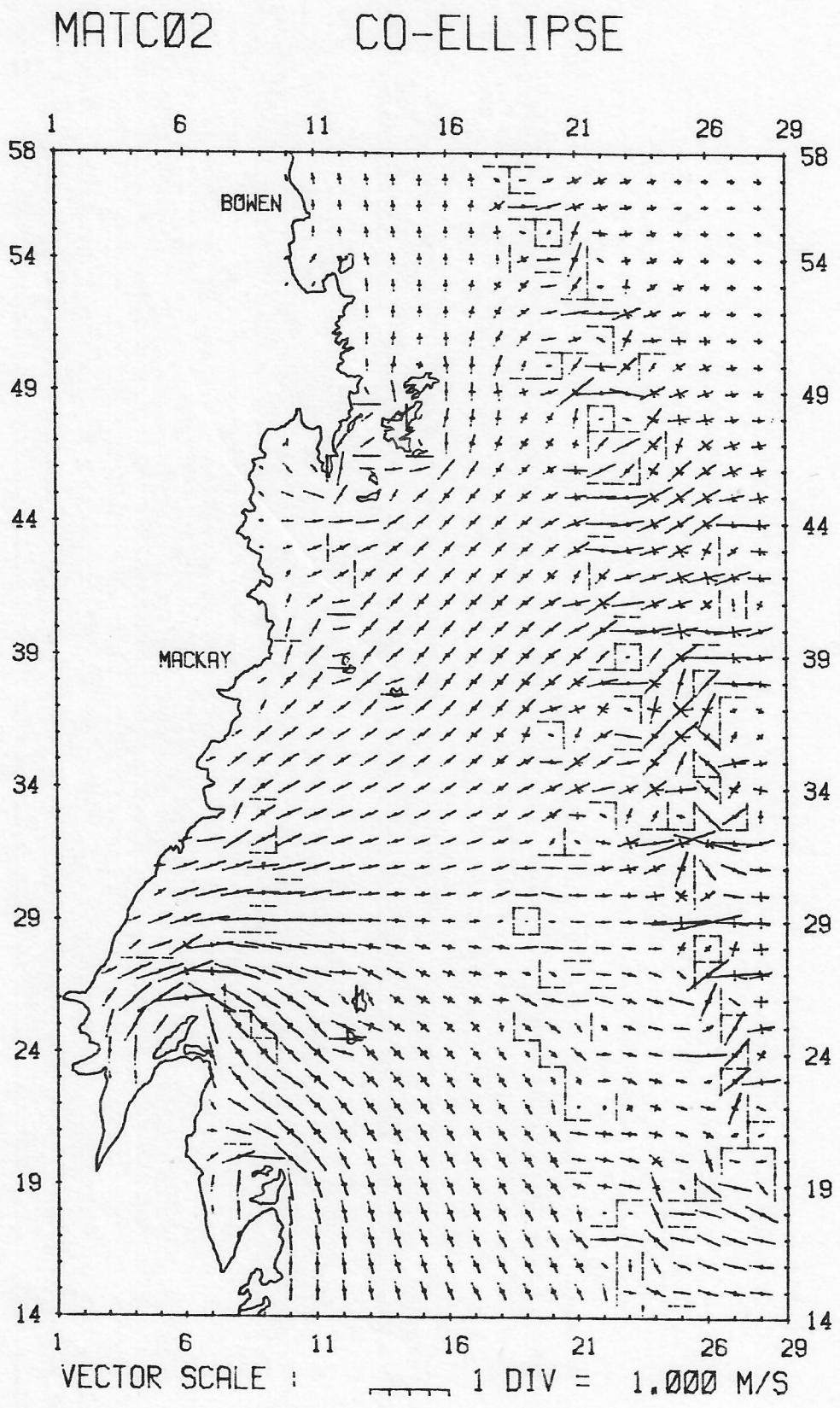

Figure 12. M_2 tidal ellipses for central window of Mackay model region.

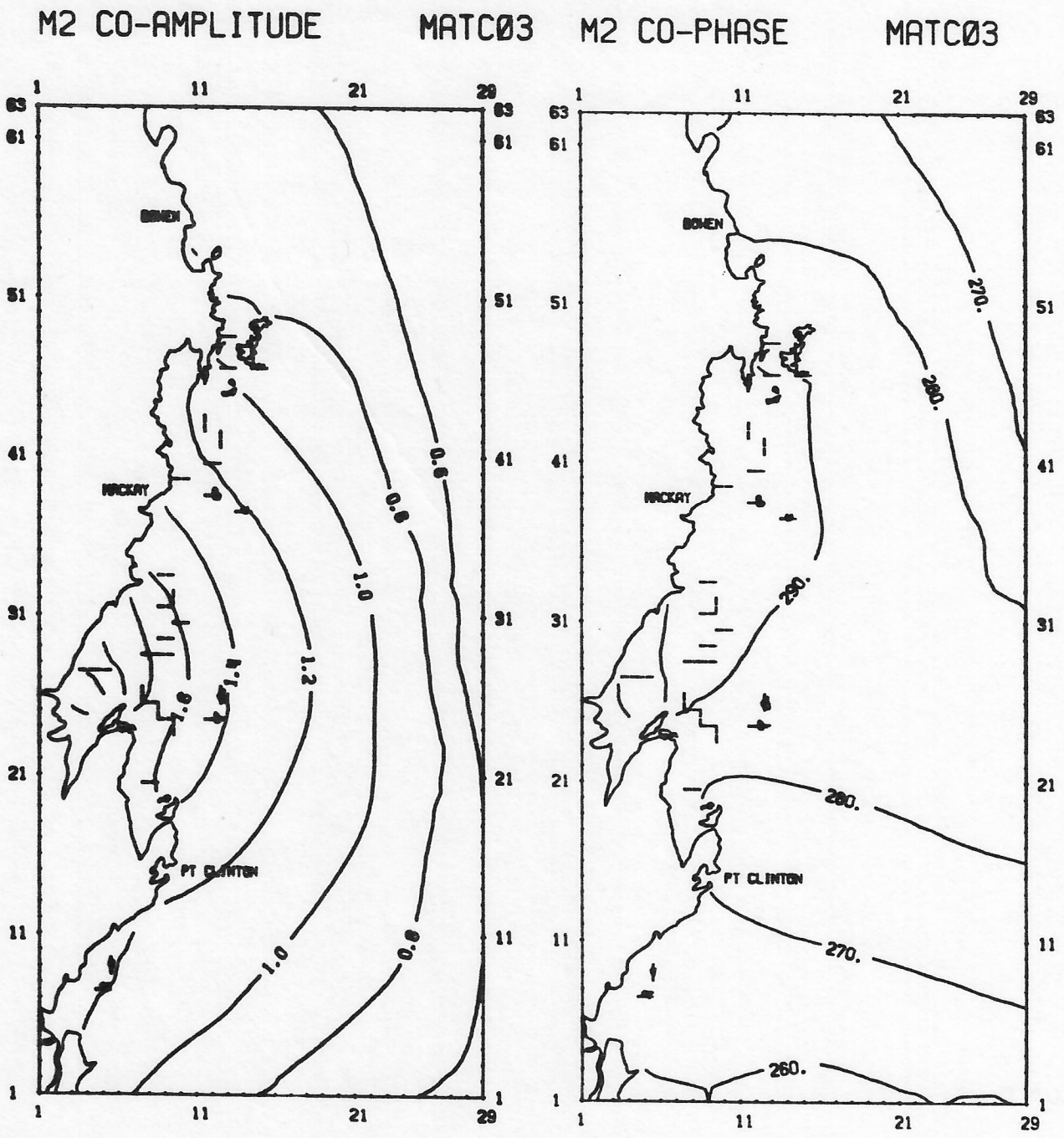

Figure 13. As for Figure 11, but with 'reef' removed.

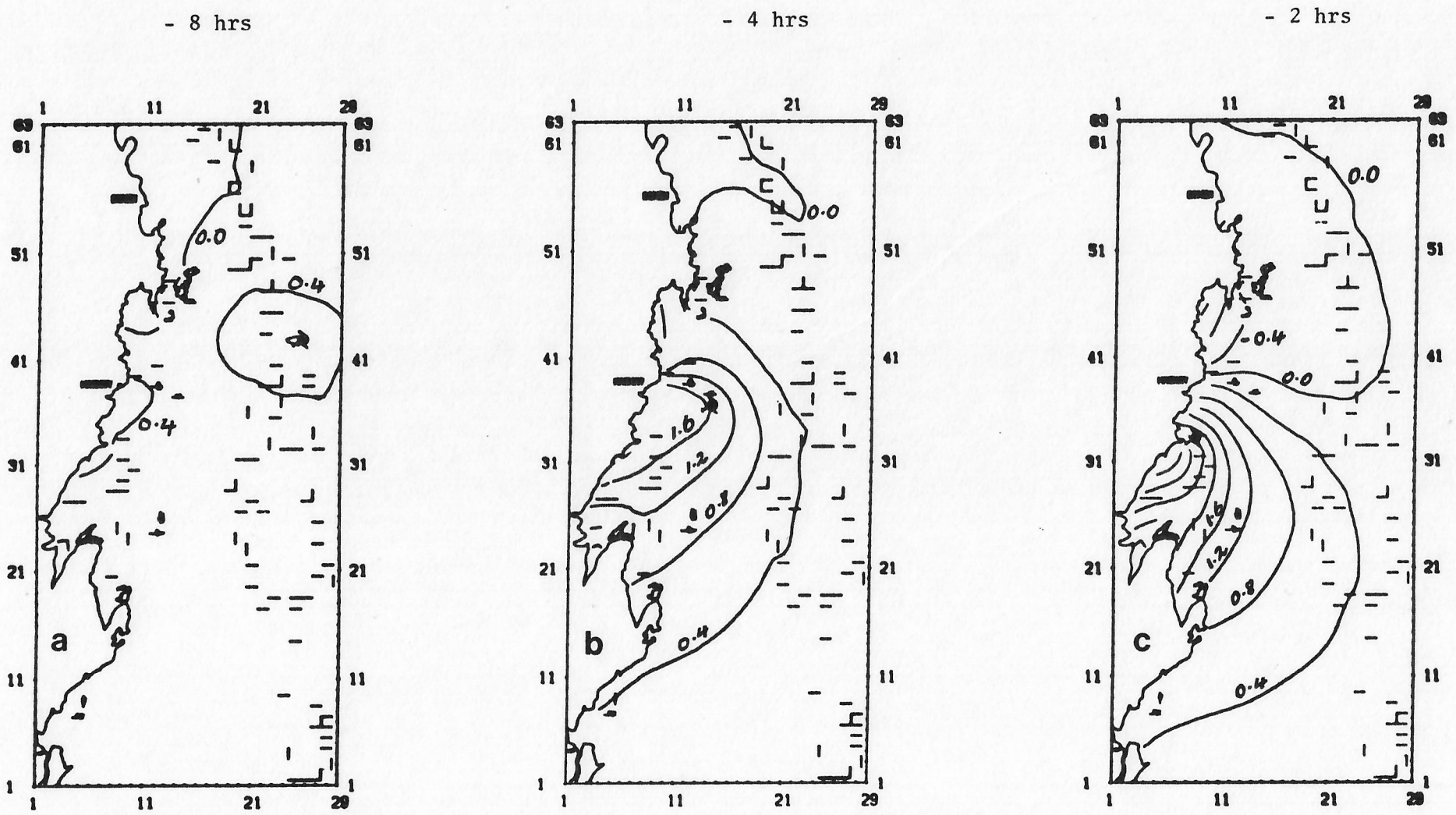

Figure 14. Sea surface elevation (metres) above MSL for surge alone simulation at times (a) t = -8 hr, (b) t = -4 hr, (c) t = -2 hr and, overleaf (d) t = -1 hr, (e) t = 0 hr, (f) t = +1 hr with respect to landfall.

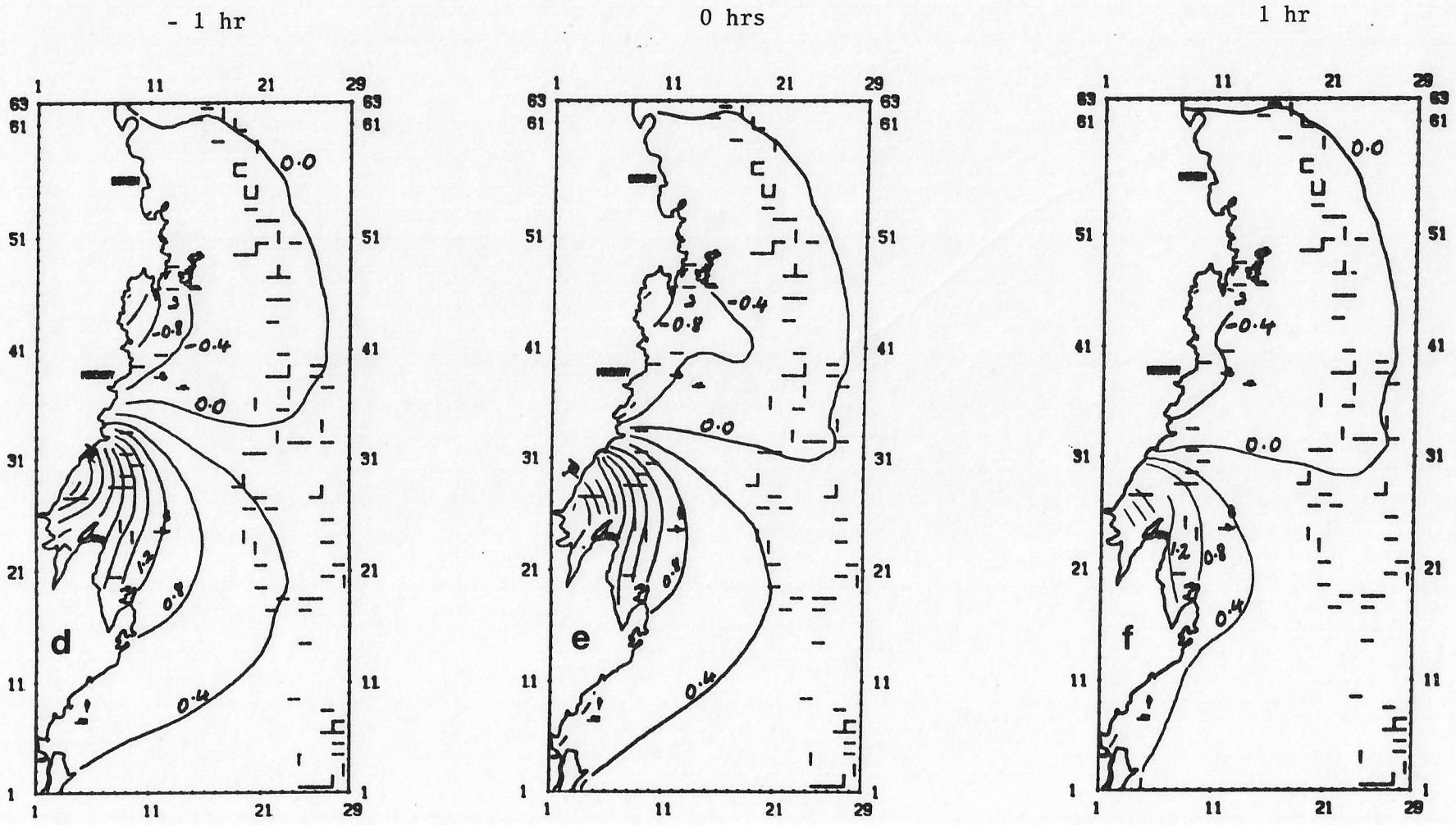

Figure 14. See previous page for caption.

- 4 hrs

- 2 hrs

0 hrs

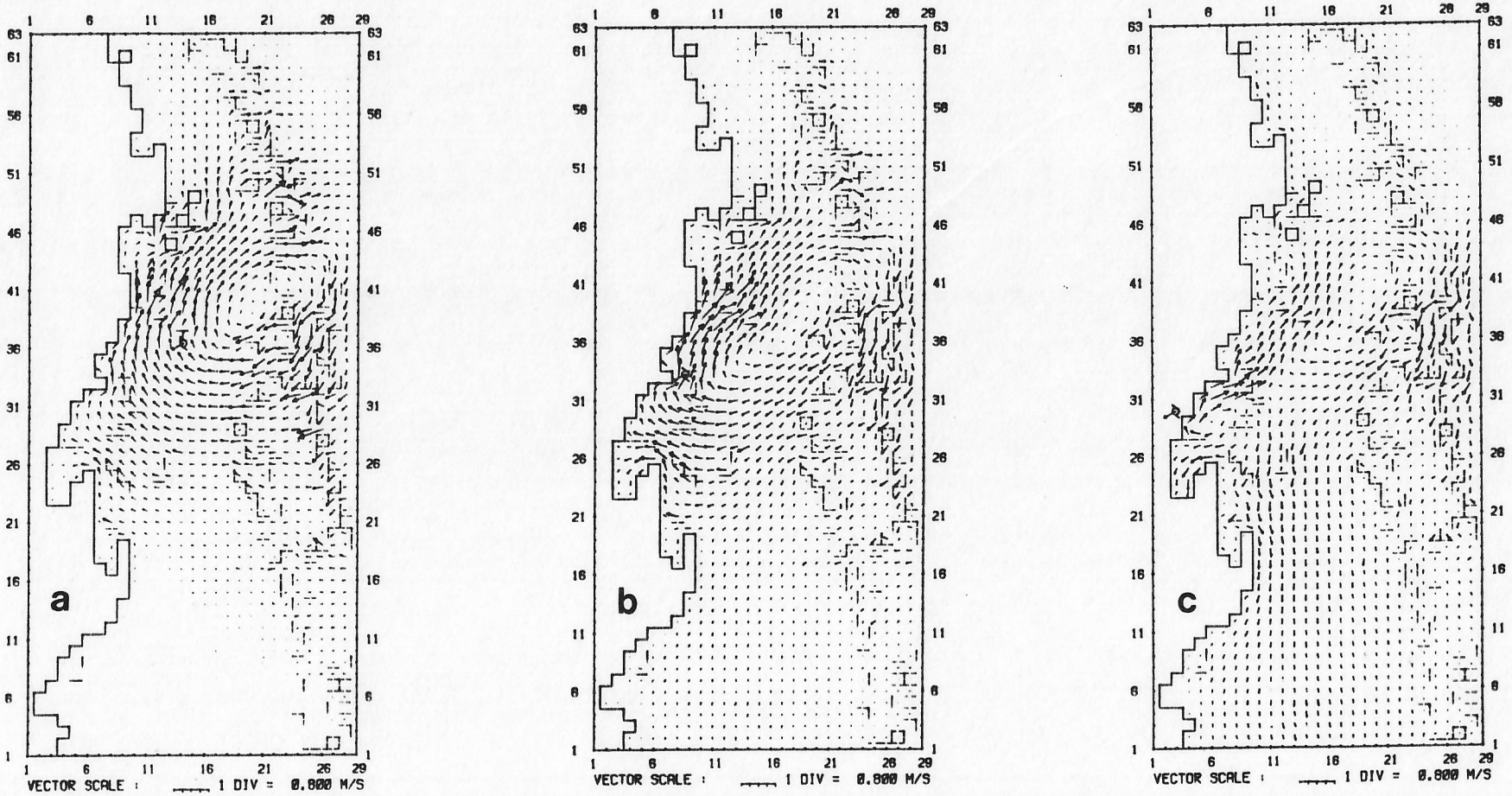

Figure 15. Depth-averaged currents for surge alone in Mackay region at times of (a) t = -4 hr, (b) t = -2 hr, (c) t = 0 hr with respect to landfall. Overleaf, (d) shows detail of the centred window region.

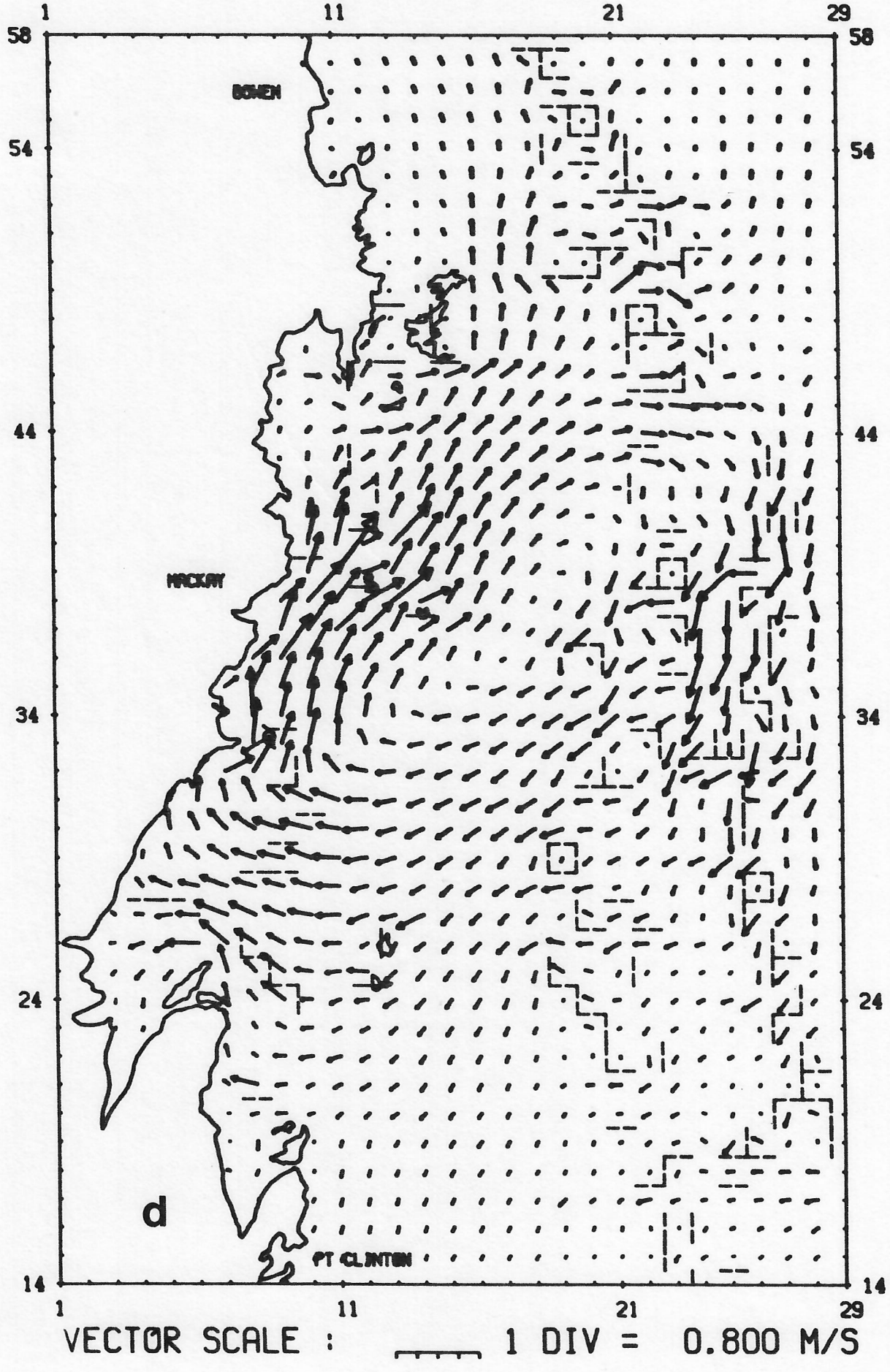

Figure 15(d). See previous page for caption.

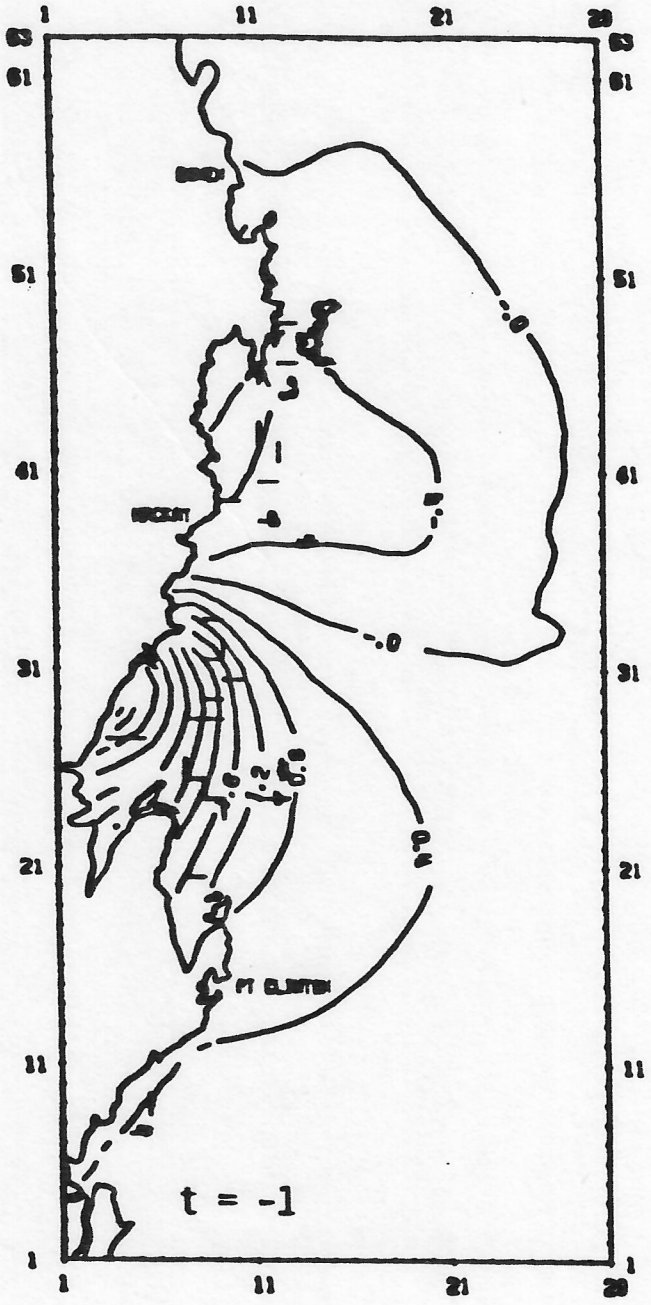

Figure 16. Storm surge water level elevation (metres) at t = -1 hr with respect to landfall, but with 'reef' removed - compare with Figure 14(d).

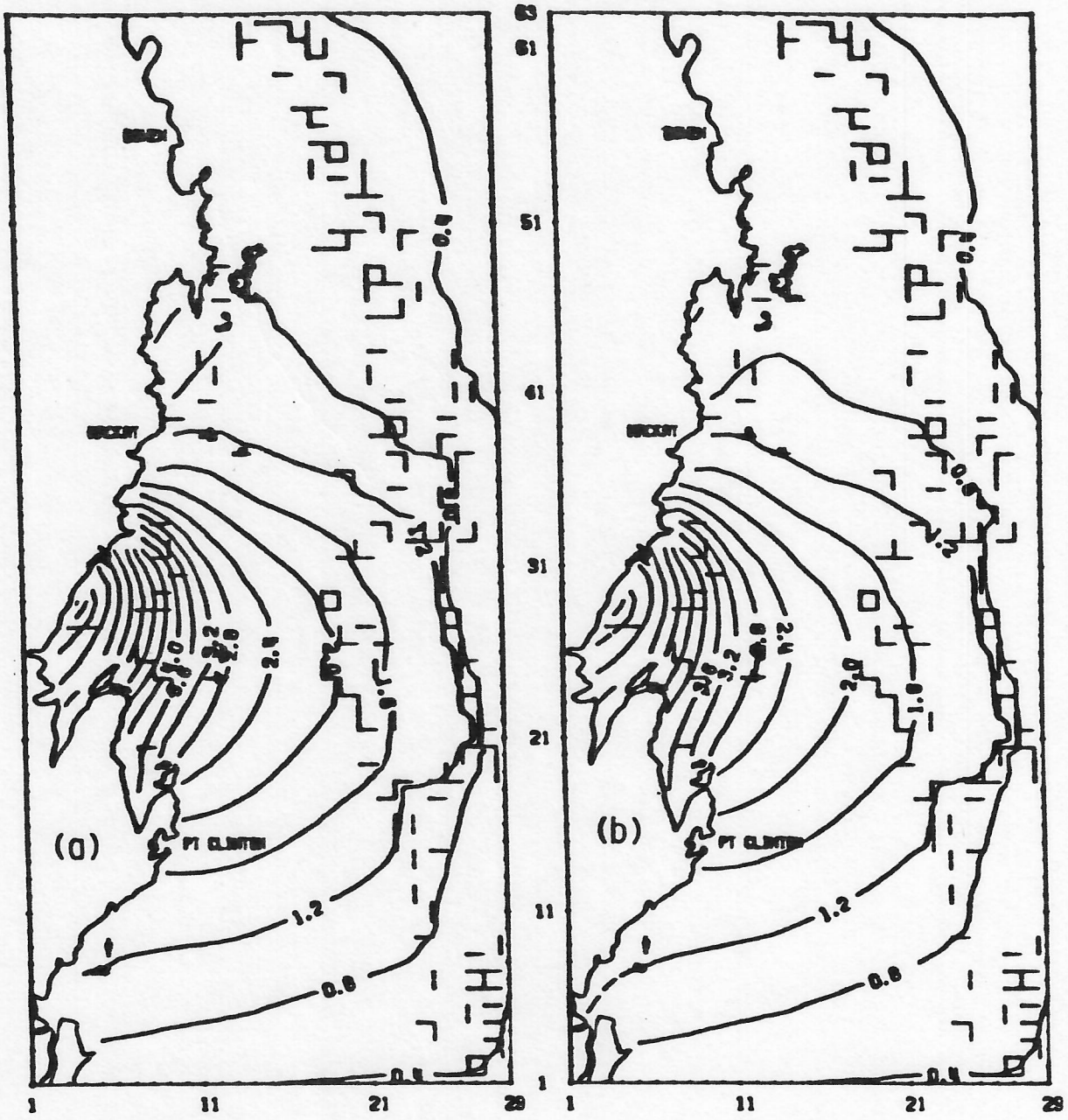

Figure 17. Comparison of surface elevations (metres) at t = -1 hr for (a) Surge + Tide, (b) combined Surge/Tide simulations.

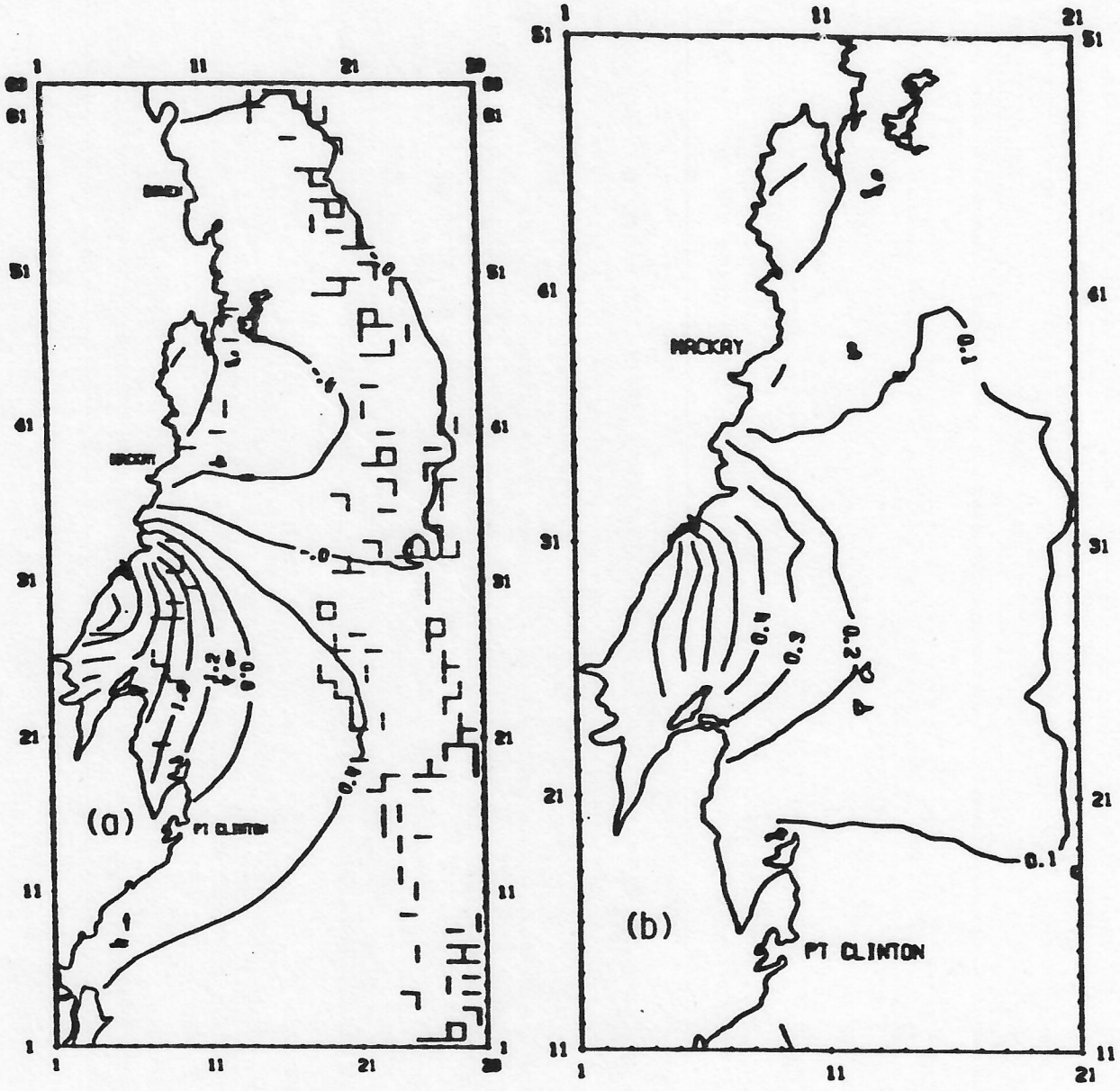

Figure 18. (a) Net surge (metres) at t = -1 hr for combined Surge/Tide; (b) Excess water elevation (metres) of Surge + Tide over Surge/Tide at t = -1 hr.

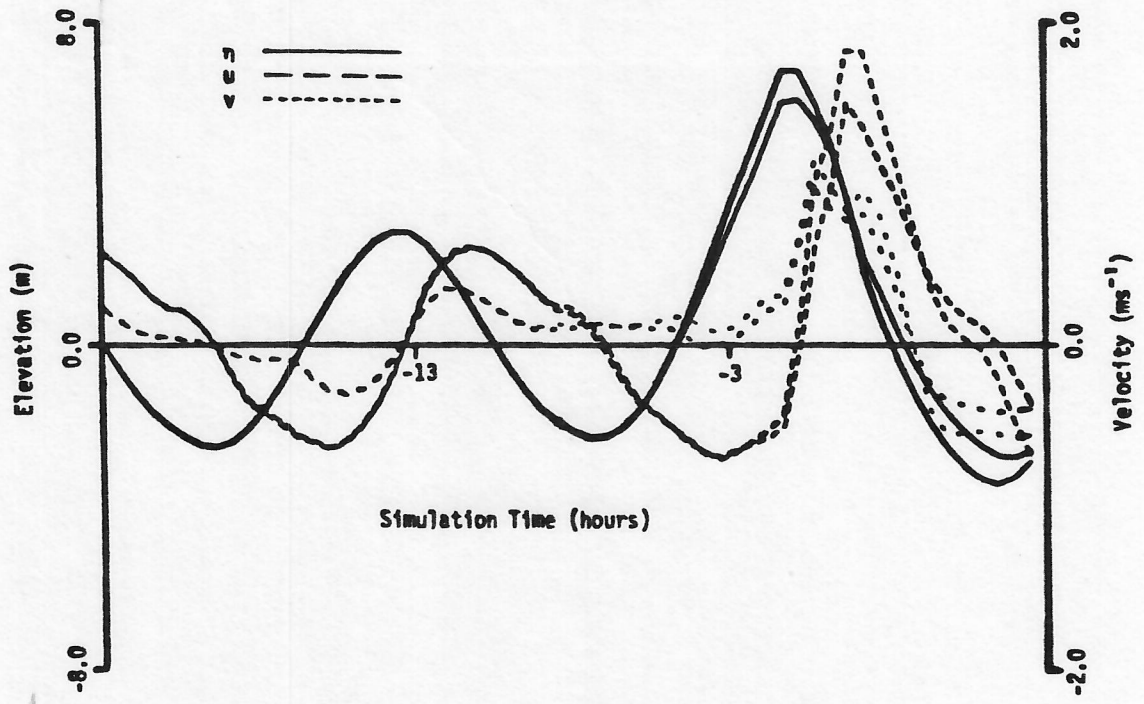

Figure 19. Time histories at grid point (5,29) of water level elevation and velocity components for both Surge + Tide and combined Surge/Tide simulations.